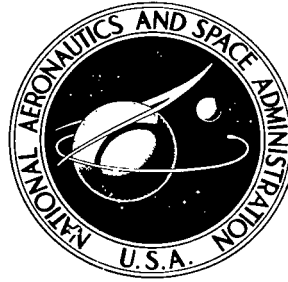


NASA TECHNICAL NOTE



NASA TN D-4433

C. 1

NASA TN D-4433

LOAN COPY: 1
AFWL (W
KIRTLAND AF



A CRITICAL EVALUATION OF
THE USE OF ULTRASONIC
ABSORPTION FOR DETERMINING
HIGH-TEMPERATURE GAS PROPERTIES

by Warren F. Ahtye
Ames Research Center
Moffett Field, Calif.



A CRITICAL EVALUATION OF THE USE OF ULTRASONIC ABSORPTION
FOR DETERMINING HIGH-TEMPERATURE GAS PROPERTIES

By Warren F. Ahtye

Ames Research Center
Moffett Field, Calif.

NATIONAL AERONAUTICS AND SPACE ADMINISTRATION

For sale by the Clearinghouse for Federal Scientific and Technical Information
Springfield, Virginia 22151 - CFSTI price \$3.00

TABLE OF CONTENTS

	<u>Page</u>
SUMMARY	1
INTRODUCTION	2
SYMBOLS	3
CLASSICAL ABSORPTION AND ZERO FREQUENCY SPEED OF SOUND	7
ULTRASONIC ABSORPTION DUE TO THERMAL RADIATION	15
ULTRASONIC ABSORPTION DUE TO RELAXATION EFFECTS	20
ABSORPTION MEASUREMENTS IN OTHER GASES	34
CONCLUDING REMARKS	38
REFERENCES	41
FIGURES	47

A CRITICAL EVALUATION OF THE USE OF ULTRASONIC ABSORPTION
FOR DETERMINING HIGH-TEMPERATURE GAS PROPERTIES

By Warren F. Ahtye

Ames Research Center

SUMMARY

The usefulness of ultrasonic absorption for determining the values of high-temperature gas properties has been examined critically. The sources of ultrasonic absorption considered are: viscosity and thermal conductivity (classical absorption), thermal radiation, and relaxation effects due to dissociation, ionization, and electronic excitation by atomic collisions. The absorption values for argon and nitrogen were calculated in an attempt to explain the large disparity between classical values and those measured by Carnevale in a series of electric arc experiments. Ultrasonic absorption in oxygen and in hydrogen was also examined.

The calculations show that it is possible to measure the transport coefficients of argon and hydrogen for two states. The first occurs when either gas is predominantly in the atomic state. The second state occurs when either gas is mainly comprised of single ions and electrons. The transport coefficients of nitrogen and oxygen cannot be measured with any degree of accuracy at any temperature because of the masking of the classical absorption by relaxation effects.

The calculations show that the ultrasonic absorption associated with thermal radiation is so minute that the absorption technique is incapable of measuring total radiative intensities of atmospheric gases even at temperatures sufficiently high that single ionization occurs.

The differences between the classical values of the ultrasonic absorption and those measured by Carnevale can be explained by relaxation phenomena. For example, the anomalous absorption measured in argon is attributed to the finite reaction rate for ionization. From this it is concluded that ultrasonic absorption can be used for accurately measuring the predominant ionization rate constant of argon. Ionization relaxation cannot account for the bulk of the anomalous absorption in nitrogen. It is shown that most of the anomalous absorption can be attributed to collisional excitation of the bound electrons in nitrogen atoms, but only if a high collisional efficiency exists. The reasonableness of the required collisional efficiency cannot be checked at the present time as the excitation cross sections have not been calculated or measured directly.

INTRODUCTION

A knowledge of transport properties, reaction rates, and radiative properties of atmospheric gases is essential for studying the heating problem of hypervelocity reentry vehicles at high altitudes. There has been an abundance of predicted values of these properties. However, in certain instances, the values are based on theories which are known to be only crude approximations to the actual phenomena. Unfortunately, there has been a paucity of experimental values for certain of these properties at conditions corresponding to those near the stagnation point of a hypervelocity vehicle. For example, Maecker's arc plasma technique is presently the only reliable one for measuring thermal conductivity where radiative properties are negligible (ref. 1). Lin and Kantrowitz's shock tube technique is presently the only method available for measuring d.c. electrical conductivity (ref. 2). The outlook for the measurement of vibrational relaxation times is much better. Various techniques have been used to measure vibrational relaxation times of a number of gases up to temperatures where dissociation coupling becomes appreciable. A list of some of these experiments is given in reference 3. Dissociation rates have been determined for a number of gases at conditions where the degree of dissociation is relatively small. A summary of these experiments is given in reference 4. However, few measurements of dissociation rates or dissociative recombination rates at moderate degrees of dissociation have been obtained. A few experiments have been performed to measure the ionization rates behind shock waves where the rates are relatively small (refs. 5 to 7). However, no direct measurements of the ionizing recombination rates have been obtained. The determination of thermal radiation from high temperature gases is extremely important because radiation dominates the energy transfer for hypersonic vehicles in certain situations. Gross radiative measurements (in contrast to spectral line measurements) have been made by AVCO (ref. 8) by extending the Maecker technique to higher temperatures.

Ultrasonics has been used to measure many of the properties at low gas temperatures. For example, the viscosity and thermal conductivity of monatomic gases and the vibrational relaxation times of polyatomic gases have been measured. The results of these measurements have been reviewed by Markham, Beyer, and Lindsay (ref. 9), Richardson (ref. 10), and Herzfeld and Litovitz (ref. 11). The experimental values of ultrasonic absorption due to transport coefficients and those due to vibrational relaxation agree quite well with theory. However, theory also predicts ultrasonic attenuation due to two additional effects: chemical reactions (refs. 12 and 13), and radiative heat transfer (refs. 14 and 15). Both effects are essentially absent in low-temperature atmospheric gases.

During the last few years, Carnevale et al. used ultrasonics at increasingly higher temperatures (ref. 16). Their primary objective was to determine experimentally the transport properties (i.e., the "sum" of the viscosity plus thermal conductivity) of high-temperature gases, both monatomic and diatomic, in the range between 3,000° and 15,000° K. They accomplished this objective by measuring the attenuation of ultrasonic pulses in the gas, then relating the attenuation to the transport coefficients by the Stokes-Kirchoff relation

(ref. 9). The validity of this approach for measuring transport coefficients at near room temperature has been established by many experiments (ref. 9). Carnevale's initial experiments were conducted with argon in an oven and a shock tube at temperatures from 300° K to a maximum of 10,000° K, where the degree of ionization is still low (2 percent). The experimentally determined attenuations (i.e., the experimentally determined viscosities and thermal conductivities) were within 10 percent of the predicted values over the entire range of temperatures. Subsequent experiments were conducted with nitrogen heated by various types of electric arcs over a temperature range where complete dissociation was attained (9,000° K), followed by partial ionization (12,000° K where the degree of ionization was 24 percent). At temperatures above 7,000° K the measured attenuations were roughly five times as large as the attenuations based on predicted values of viscosity and thermal conductivity. The cause for this much larger attenuation had not been satisfactorily explained.

The purpose of the present paper is to critically evaluate ultrasonic absorption for determining high-temperature gas properties. The first part of the paper deals with the "classical" absorption due to viscosity and thermal conductivity. The existing relationship between transport coefficients and ultrasonic attenuation are reexamined for a reacting gas. This is necessary since the relationship was specifically derived for a nonreactive gas (ref. 17). The classical absorption and dispersion for nitrogen and argon are then calculated. The absorption components due to viscosity and thermal conductivity are compared to determine whether an ultrasonic experiment can simultaneously yield accurate values for both transport coefficients. In the second part of the paper an attempt is made to explain the anomalous absorption found in Carnevale's experiments. The approach is to calculate the ultrasonic attenuation due to such phenomena as chemical relaxation and radiative heat transfer. The calculations are necessarily order-of-magnitude calculations, because: (1) certain high-temperature properties are not known to a good degree of accuracy, and (2) coupling effects (e.g., the effect of vibrational relaxation on dissociation relaxation) are not included because of the complexity of such processes. Consequently, the total ultrasonic absorption is assumed to be the sum of the absorptions due to the individual effects. The importance of explaining the anomalous absorption should be emphasized, for if the absorption can be attributed to a single phenomenon (e.g., chemical relaxation), it may be possible to use an ultrasonic experiment to determine a high-temperature gas property (e.g., chemical reaction rates) other than the transport coefficients. This approach appears to be feasible since the magnitude of the anomalous absorption is at least four times as large as the classical absorption.

SYMBOLS

- a speed of light
- A argon atom

A^+	argon ion
c	speed of sound
c_0	speed of sound at zero frequency
c_p	specific heat per unit mass at constant pressure
c_v	specific heat per unit mass at constant volume
\underline{d}	forcing potential
d_{ij}	rate of deformation tensor
D_{ij}	multicomponent diffusion coefficient
D_i^T	thermal diffusion coefficient
e	electron
E	reaction energy
f	ultrasonic frequency
f_E	fraction of sufficiently energetic collisions
\underline{F}	external force vector per unit mass
g_i	degeneracy of the i th quantum state
h	enthalpy per unit mass, also normalized radiative absorption coefficient
I	ionization potential
J_b	black-body function
J_λ	spectral emission coefficient
k	Boltzmann's constant, also acoustic propagation constant, $\frac{\omega}{c}$
k_d	dissociation rate coefficient
k_i	ionization rate coefficient
k_0	acoustic propagation constant, $\frac{\omega}{c_0}$
m	mass
M	molecular weight

n	number density
N	nitrogen atom
N_2	nitrogen molecule
N^+	nitrogen ion
p	pressure
P	steric factor
\underline{q}	heat flux vector
Q	radiation coefficient
\underline{r}	position vector
R	universal gas constant
Re	real part of a complex quantity
s	entropy per unit mass
S'	reciprocal of the normalized radiation coefficient, $\frac{Q}{\omega}$
t	time
T	temperature
\underline{u}	mass average velocity
U	reaction rate near equilibrium
v	volume per unit mass
V	volume
\overline{V}_s	diffusion velocity
W	heat of reaction
\underline{x}	position vector
x_i	mol fraction of species i
X	frequency number
\underline{X}_s	external force
Y	thermo-viscous number

z	collision frequency
Z	compressibility
α	ultrasonic absorption coefficient
β	thermal expansion coefficient
γ	ratio of specific heats, $\frac{c_p}{c_v}$
δ	finite increment
ϵ	internal energy per unit mass
ϵ_i	energy of the i th quantum state
η	viscosity coefficient
η_B	bulk viscosity
λ	coefficient of thermal conductivity
λ_d	coefficient of thermal conductivity due to thermal diffusion
λ_r	coefficient of thermal conductivity due to chemical reaction, also wavelength of electromagnetic radiation
λ_s	ultrasonic wavelength
λ_t	coefficient of thermal conductivity due to atomic collisions
λ_{total}	total coefficient of thermal conductivity
μ	radiative absorption coefficient
ν	viscosity number
ν_{ij}	stoichiometric coefficient
ν_j	the sum of the stoichiometric coefficients for a given reaction
ρ	density
σ	rigid sphere collision diameter, also Stefan-Boltzmann constant
τ	relaxation time
Φ_η	viscous dissipation function
ω	ultrasonic angular frequency, $2\pi f$

$\Omega^{(2,2)*}$ ratio of viscosity cross section to hard sphere cross section
 [] mol concentration

Subscripts

av average value
 class classical value
 diss dissociation
 elast elastic collision
 exc collisional excitation of bound electrons
 i ith cartesian component, also ith species
 ion ionization
 o equilibrium value
 p constant pressure process
 rad thermal radiation
 react chemical reaction
 relax relaxation
 s constant entropy process, also particles of type s
 tran transition
 v constant volume process
 vib vibration
 η viscosity
 λ thermal conductivity

CLASSICAL ABSORPTION AND ZERO FREQUENCY SPEED OF SOUND

The value of the ultrasonic absorption due to viscosity and thermal conductivity represents the minimum value of absorption for any gas, monatomic or polyatomic, reactive or nonreactive. This absorption is usually called

the classical absorption, and is attained in the limit of extremely low frequencies where nonequilibrium effects are allowed to relax completely within the period of an ultrasonic wave. The value of the corresponding zero frequency speed of sound represents the minimum speed of sound for any gas state.

The relationship between the classical absorption coefficient and the transport coefficients for a nonreactive monatomic gas is given in reference 17 as

$$\alpha_{\text{class}} = \frac{\omega^2}{2\rho c_0^3} \left[\frac{4}{3} \eta + (\gamma - 1) \frac{\lambda}{c_p} \right] \quad (1)$$

Equation (1) is called the Stokes-Kirchoff relation. For this case the specific heat, c_p , and the ratio of specific heats, γ , are constants. In addition both the viscosity, η , and the thermal conductivity, λ , are inversely proportional to the atom-atom collision cross section. As a result, the ratio of the thermal conductivity to the viscosity is the constant

$$\frac{\lambda}{\eta} = \frac{5}{2} c_v \quad (2)$$

(ref. 18). Consequently, using measured absorption coefficients in equations (1) and (2) permits the accurate determination of the viscosity and thermal conductivity. Such measurements also yield values for the atom-atom collision cross sections, since kinetic theory has established an accurate relationship between the cross sections and the transport coefficients.

It is not obvious that equation (1) can be used for a reactive gas since γ and c_p are no longer constants. Rather, they are characterized by relatively large changes with increasing temperature because of vibrational excitation, electronic excitation, dissociation, and ionization, as shown in figures 1 and 2. The argon data are taken from references 18 and 19 and the nitrogen data are taken from references 18 and 20. As a result of these changes, it is necessary to reexamine the assumptions underlying the exact equations describing the propagation of sound. A thorough review of these assumptions for a single component nonreactive gas was given by Hunt in reference 17. Hunt states "The motions of a fluid medium that comprise sound waves are governed by equations that include: (a) a continuity equation expressing the conservation of mass, (b) a force equation expressing the conservation of momentum, (c) a heat-exchange equation expressing the conservation of energy, and (d) one or more defining equations expressing the constitutive relations that characterize the medium and its response to thermal or mechanical stress." The overall continuity equation for a single component nonreactive gas is

$$\frac{\partial \rho}{\partial t} + u_i \frac{\partial \rho}{\partial x_i} + \rho \frac{\partial u_i}{\partial x_i} = 0 \quad (3)$$

where the subscript i is the coordinate index. The equation of motion is

$$\rho \frac{\partial u_i}{\partial t} + \rho u_j \frac{\partial u_i}{\partial x_j} = \rho F_i - \frac{\partial p}{\partial x_i} + \frac{\partial}{\partial x_j} (\eta' d_{kk} \delta_{ij} + 2\eta d_{ij}) \quad (4)$$

where d_{ij} is the rate of deformation tensor, and η' is the "second" or dilatational viscosity coefficient. (Note that a repeated subscript denotes a summation.) The equation of energy balance is

$$\rho c_v \left(\frac{\partial T}{\partial t} + u_i \frac{\partial T}{\partial x_i} \right) + \rho c_v \frac{\gamma - 1}{\beta} \frac{\partial u_i}{\partial x_i} + \frac{\partial q_i}{\partial x_i} - \phi_\eta = 0 \quad (5)$$

where β is the coefficient of thermal expansion (see eq. (17)), and ϕ_η is the viscous dissipation function. Note that Hunt has omitted the external force term in the energy equation. The heat flux vector, q_i , is expressed as the sum of a conductive component and a radiative component. These two components are expressed by Hunt in the form

$$(q_i)_{\text{cond}} = -\lambda \frac{\partial T}{\partial x_i} \quad (6)$$

$$\frac{\partial}{\partial x_i} (q_i)_{\text{rad}} = \rho c_v Q (T - T_0) \quad (7)$$

The equations of change for a chemically reactive multicomponent monatomic gas are given in reference 21 (p. 698). The mass conservation equation from reference 21 is identical with equation (3). The momentum conservation equation from reference 21 differs from equation (4) only in that the force term in the former is a sum over all species, $\sum_s n_s m_s F_s$. The difference is academic as external forces are not considered in the analyses given here. The energy conservation equation from reference 21 is equivalent to equation (5), with one exception. In reference 21, the conductive heat flux vector is defined as

$$(\underline{q})_{\text{cond}} = -\lambda_t \frac{\partial T}{\partial \underline{r}} + \sum_s n_s h_s \bar{\underline{v}}_s - nkT \sum_s \frac{1}{n_s m_s} D_s^T \underline{d}_s \quad (8)$$

where $\bar{\underline{v}}_s$ is the diffusion velocity vector for species s , the quantity D_s^T is the thermal diffusion coefficient, and \underline{d}_i is a "forcing potential" vector defined as

$$\underline{d}_s = \frac{\partial x_s}{\partial \underline{r}} + \left(x_s - \frac{n_s m_s}{\rho} \right) \frac{\partial \ln p}{\partial \underline{r}} - \left(\frac{n_s m_s}{p \rho} \right) \left(\frac{\rho}{m_s} \underline{x}_s - \sum_s n_s \underline{x}_s \right) \quad (9)$$

where \underline{X}_s is the external force acting on the s th particle. The first component of \underline{q} contains the translational thermal conductivity,¹ λ_t , and is the only component explained by simple kinetic theory (ref. 22). This component exists for a pure gas and a multicomponent gas. The second component is the heat flux due to diffusion of enthalpy including chemical enthalpy. The last component is the heat flux due to thermal diffusion. Unfortunately, no simple physical picture can describe this mode of heat transport. The last two components exist only for a multicomponent gas.

Brokaw (ref. 24) derived an expression for the reactive component of a dissociating gas in the form of equation (6). For an ionizing gas both the reactive and thermal diffusive components must be taken into account (ref. 25). Ahtye (ref. 26) derived an expression for these two components in the form of equation (6). As a result, the convective heat flux vector for dissociating and ionizing gases can be expressed in terms of an effective or total coefficient of thermal conductivity. Consequently, if one wishes to calculate the classical absorption by using the general approach described by Hunt, then one must use the total thermal conductivity rather than just the translational component.

The remaining step in this reexamination is to determine if the constitutive equations in the classical approach are valid for a reactive gas. The approach of reference 17 specifies the state of the fluid by using the specific entropy and the specific volume, in terms of which the thermodynamic pressure and temperature, and the specific heats can be defined

$$\epsilon = \epsilon(s, v) \quad (10)$$

$$p = - \left(\frac{\partial \epsilon}{\partial v} \right)_s \quad (11)$$

$$T = \left(\frac{\partial \epsilon}{\partial s} \right)_v \quad (12)$$

$$c_p = T \left(\frac{\partial s}{\partial T} \right)_p \quad (13)$$

$$c_v = T \left(\frac{\partial s}{\partial T} \right)_v \quad (14)$$

$$\gamma \equiv \frac{c_p}{c_v} \quad (15)$$

¹It is possible to include the effects of vibrational-translational energy interchange by including a thermal conductivity correction (ref. 23).

An additional relationship was used to reduce the number of parameters in the absorption equation. This relationship is

$$T\beta^2 c_o^2 = (\gamma - 1)c_p \quad (16)$$

where β , the coefficient of thermal expansion, is defined as

$$\beta = \rho \left(\frac{\partial v}{\partial T} \right)_p \quad (17)$$

Equations (11) and (12) are forms of the first law of thermodynamics, which hold for any system (e.g., a reactive gas). Equations (13) and (14) follow from the first and second laws of thermodynamics which hold for any system. Equation (16) can be verified for a reactive gas by using the relations in reference 27. Consequently, the thermodynamic properties for a reactive gas, which include the effect of large energy changes due to chemical reactions, should be used in the calculation of the classical absorption.

Since the conservation equations in reference 17 are valid for a multi-component reactive gas, then the derivation there of the expression for the absorption coefficient is also valid. The expression for the absorption coefficient is obtained by linearizing the conservation equations. The result is a complicated expression for the complex propagation constant, $\alpha + ik$, due to the combined effects of viscous shear, conduction and radiative heat transfer. In order to obtain an expression for the absorption coefficient, the three effects must be separated. Hunt's approach is to first examine the combined effects of viscous shear and conductive heat transfer (classical absorption), then to examine the effect of radiative heat transfer. The classical absorption will be discussed in this section. The absorption due to radiative heat transfer will be discussed in a subsequent section.

Hunt expressed the classical absorption coefficient and the corresponding dispersion relation as a power series expansion in terms of a dimensionless frequency number, X . Only the first two terms in the expansion are used. The absorption expression is

$$\begin{aligned} \frac{\alpha_{\text{class}}}{k_o} = & \frac{1}{2} X[1 + (\gamma - 1)Y] - \frac{1}{16} X^3[5 + 35(\gamma - 1)Y \\ & + (\gamma - 1)(35\gamma - 63)Y^2 + (\gamma - 1)(5\gamma^2 - 30\gamma + 33)Y^3] \end{aligned} \quad (18)$$

where the frequency number, X , is defined as

$$X = \frac{\omega \eta \nu}{\rho_o c_o^2} \quad (19)$$

and the thermo-viscous number Y is defined as

$$Y = \frac{\lambda_{\text{total}}}{\eta \nu c_p} \quad (20)$$

where ν is a viscosity number defined as

$$\nu = \frac{4}{3} + \frac{\eta_B}{\eta} \quad (21)$$

where η_B is the bulk viscosity. The first term on the right side of equation (18) corresponds to the Stokes-Kirchoff relation (eq. (1)). It is merely the sum of the separate effects of viscosity and thermal conductivity. The second term represents the coupling between viscosity and thermal conductivity. The dispersion relation is

$$\left(\frac{c}{c_0}\right)^2 = 1 + \frac{1}{4} X^2 [3 + 10(\gamma - 1)Y - (\gamma - 1)(7 - 3\gamma)Y^2] \quad (22)$$

Hunt states that equations (18) and (22) "can be used with confidence for almost any values of γ and Y so long as the frequency is low enough to keep $X < 0.1$, and for a somewhat wider range of X when certain restrictions on γ and Y are satisfied."

Equations (18) and (22) will now be used to calculate the classical absorption and corresponding dispersion occurring in the reacting gas of reference 16. The independent variables X and Y correspond to a 1 Mc ultrasonic wave propagating through reactive nitrogen, or argon, at a pressure of 1 atmosphere and at temperatures varying from 300° to 12,000° K. The calculations are extended to 20,000° K in order to predict the absorption and dispersion of fully ionized nitrogen and argon. The thermodynamic properties of nitrogen are taken from references 18 and 20 and those of argon from references 18 and 19. The pertinent properties, Z , c_p , and c_0 are shown in figures 1, 3, and 4. The compressibility, Z , is used to calculate the density

$$\rho = \frac{pM_0}{ZRT} \quad (23)$$

where M_0 is the molecular weight per mole of the initial particle (i.e., undissociated nitrogen molecule or neutral argon atom). The reference speed of sound, c_0 , defined as the asymptotic value at zero frequency, is obtained from the dimensionless speed-of-sound parameter,

$$\frac{c_0^2 \rho}{p} = \gamma \frac{1 + \left(\frac{T}{Z}\right) \left(\frac{\partial Z}{\partial T}\right)_\rho}{1 + \left(\frac{T}{Z}\right) \left(\frac{\partial Z}{\partial T}\right)_p} \quad (24)$$

Note that this expression differs from the expression

$$(c_0^2)_{\text{class}} \frac{\rho}{p} = \gamma \quad (25)$$

which is valid only for a nonreactive gas.

The transport coefficients of dissociating nitrogen are taken from reference 28. The transport coefficients of ionizing nitrogen were calculated by using the second-order Chapman-Enskog expressions in references 25 and 26, and the collision cross sections in references 8 and 29. These coefficients are shown in figures 5 and 6. The transport coefficients of ionizing argon are taken from references 25 and 26, and are also shown in figures 5 and 6.

The classical absorption coefficient and zero frequency speed of sound are obtained by applying the thermodynamic properties and transport coefficients to equations (18), (22), and (24). It may be instructive to first inspect typical values of X and Y to determine the validity of equations (18) and (22). These values are shown in the following table:

Gas	Temperature, °K	Percent dissociation or ionization	X	Y	XY
Nitrogen	293	0 d	1.25×10^{-3}	0.874	1.09×10^{-3}
	5,000	1.7 d	1.36×10^{-2}	.897	1.22×10^{-2}
	7,000	45.3 d	1.54×10^{-2}	.859	1.33×10^{-2}
	9,500	100 d	1.73×10^{-2}	.460	7.93×10^{-3}
	15,000	53.5 i	8.43×10^{-3}	.867	7.30×10^{-3}
	20,000	96.2 i	1.01×10^{-3}	17.2	1.74×10^{-2}
Argon	293	0 i	1.09×10^{-3}	1.13	1.21×10^{-3}
	5,000	0 i	9.10×10^{-3}	1.12	1.02×10^{-2}
	10,000	2.1 i	1.93×10^{-3}	1.02	1.96×10^{-2}
	15,000	58.6 i	5.19×10^{-3}	2.33	1.21×10^{-2}
	20,000	97.7 i	1.39×10^{-3}	44.3	6.17×10^{-2}

Several conclusions can be drawn from this table. The values of the frequency number, X , are considerably less than unity. Consequently, the expansion scheme used by Hunt is justified. The higher powers of X and XY are sufficiently small that several simplifications can be made in equations (18) and (22). First, the viscosity-conductivity coupling term (second term of eq. (18)) in the absorption equation is at least three orders of magnitude smaller than the separate effects of viscosity and thermal conductivity, so the coupling term may be neglected. Second, the dispersion effect due to viscosity and thermal conductivity (second term of eq. (22)) is of the order of 10^{-4} . Consequently, these particular dispersion effects may also be neglected.

The next step is to compare the absorption induced by viscosity with that induced by thermal conductivity. Figure 7 shows the ratio of the two absorptions, which can be expressed as

$$\frac{\alpha_\lambda}{\alpha_\eta} = (\gamma - 1)Y = (\gamma - 1) \frac{\lambda_{\text{total}}}{\eta v_{c_p}} \quad (26)$$

Three cases are shown: (1) ionizing argon, (2) dissociating nitrogen, and (3) ionizing nitrogen. For argon, the ratio $\alpha_\lambda/\alpha_\eta$ is essentially constant at temperatures below 7000° K (ionization levels below 0.001). The ratio should be constant in this region because the quantities $\lambda_{\text{total}}/\eta$, c_p , and γ are constants due to the absence of electronic excitation and ionization effects. As the ionization level increases beyond 0.001, the ratio drops rapidly, reaching a minimum of 0.2 at an ionization level of 0.1. This drop off can be attributed mainly to the rapid decrease of $\gamma - 1$ as electronic excitation and ionization effects become perceptible. At ionization levels greater than 0.5, the ratio $\alpha_\lambda/\alpha_\eta$, climbs abruptly, reaching a value of approximately 20 at the point where the gas is completely ionized. This increasing predominance of α_λ can be attributed to the sudden drop in the viscosity (fig. 6) which is caused by the large coulombic cross sections for the ion-ion interaction.

Beyond 12,000° K the temperature variation of $\alpha_\lambda/\alpha_\eta$ for ionizing nitrogen is similar to that for ionizing argon. In contrast, the variation of $\alpha_\lambda/\alpha_\eta$ for dissociating nitrogen below 12,000° K is irregular even at dissociation levels below 0.001. The initial drop is caused by the gradual excitation of the vibrational modes² of N_2 as the temperature approaches the characteristic vibrational temperature of 3,380° K. At dissociation levels beyond 0.001 (4,000° K), the ratio is further complicated by electron excitation and dissociative effects.

The accuracy with which η or λ_{total} or both can be determined in an ultrasonic experiment is dictated by the values of $\alpha_\lambda/\alpha_\eta$ described above. For example, if both η and λ_{total} depend only upon a single collision cross section (as they do for a monatomic gas at temperatures sufficiently low that ionization effects are not present), then η and λ_{total} can be measured simultaneously. Unfortunately, the physical situation in a diatomic gas or any reacting gas is much more complex. For example, the transport coefficients of a partially ionized gas are dependent upon six different collision cross sections. Each of these cross sections is weighted differently in the expressions for the viscosity and the total thermal conductivity. As a result, the ratio of the total thermal conductivity to the viscosity is no longer a well-established quantity independent of the temperature. However, either one of the two transport coefficients can still be measured with a fair amount of accuracy, provided the attenuations due to the other transport coefficient (and to any relaxation phenomena) are comparatively small. This occurs when the ratio $\alpha_\lambda/\alpha_\eta$ is either much less or much greater than unity.

On the basis of the previous paragraph we can determine which transport coefficient can be obtained from ultrasonic absorption measurement for a given temperature region. Argon will be examined first. From figure 7, it is seen that it should be possible to accurately measure λ_{total} and η simultaneously for temperatures up to 7,000° K because the ratio of the two quantities is

²The values of α and c_0 described in this section do not include the effects of vibrational relaxation.

well established by kinetic theory. The measurements by Carnevale (ref. 16) at these lower temperatures are shown in figure 8(a). In the intermediate region between 7,000° and 10,000° K a direct determination of either λ or η does not appear to be practical since the ratio $\lambda_{\text{total}}/\eta$ is not known with the same degree of accuracy, and since the ratio $\alpha_\lambda/\alpha_\eta$ is still relatively large. At temperatures from 10,000° to 13,000° K (0.2 ionization level) it should be possible to measure the viscosity coefficient for argon fairly accurately because of the predominance of α_η . For example, if an assumed value of λ_{total} were in error by 50 percent, this would induce an error of 10 percent in the measurement of η . In the region of 15,000° K (0.5 ionization level) a great amount of interest has been focused on the thermal conductivity due to the presence of a large peak (fig. 5). This peak is the result of diffusion of chemically reactive species (i.e., reactive component of the thermal conductivity). However, there is no accompanying sudden rise in the ratio $\alpha_\lambda/\alpha_\eta$ because the peak in λ_{total} is cancelled by the peak in c_p (eq. (26)). Not even the viscosity can be obtained in this region since $\alpha_\lambda/\alpha_\eta$ is near unity. At temperatures above 20,000° K where all the particles are charged, α_λ is greater than α_η by at least an order of magnitude. This occurs because of the sharp drop in the viscosity coefficient (fig. 6) due to the large coulomb cross section for the ion-ion interaction. It should therefore be possible to measure the thermal conductivity of a plasma by the ultrasonic absorption technique.

The thermodynamic and transport properties of partially ionized nitrogen and partially ionized argon have roughly the same temperature variations (figs. 1 to 6), causing very similar temperature variations of $\alpha_\lambda/\alpha_\eta$ (fig. 7). Consequently, the conclusion stated in the previous paragraph for argon measurements should hold for nitrogen measurements at temperatures greater than 10,000° K. At temperatures below 10,000° K, the temperature variation of $\alpha_\lambda/\alpha_\eta$ for nitrogen is entirely different. The regularity found in argon is absent, and the magnitude of $\alpha_\lambda/\alpha_\eta$ is lower by a factor of 2 to 3 throughout most of this temperature range. At temperatures up to 6,000° K this difference can be attributed to the changes in $\gamma - 1$ due to the additional rotational and vibrational modes of the molecule. From an examination of the classical absorption alone, it can be concluded that it is possible to measure the viscosity of nitrogen from room temperatures up to 15,000° K by the ultrasonic absorption technique because $\alpha_\lambda/\alpha_\eta$, though irregular, is so low.

Of course, the conclusions in this section are based on the premise that other sources of ultrasonic absorption are unimportant. Consequently, these conclusions will be modified after other sources are discussed in subsequent sections.

ULTRASONIC ABSORPTION DUE TO THERMAL RADIATION

The results of Carnevale's high-temperature experiments (ref. 16) are shown in figure 8. These experiments were conducted at a pressure of

1 atmosphere. Measurements below $5,000^{\circ}$ K were obtained in an oven, whereas those above $5,000^{\circ}$ K were obtained with various types of electric arcs. The initial experiments, conducted with argon at temperatures from 300° to $10,000^{\circ}$ K are shown in figure 8(a) in the form of the viscosity coefficient (eqs. (1) and (2)). It can be seen that the agreement between the measured and calculated values of the viscosity is excellent up to $7,000^{\circ}$ K, indicating that ultrasonic absorption can accurately measure transport coefficients of nonreactive monatomic gases up to extremely high temperatures.

Additional argon measurements up to $18,000^{\circ}$ K in figure 8(b) show considerable anomalous absorption (i.e., difference between the measured and classical values) above $10,000^{\circ}$ K where ionization effects become important. The disparity is even greater for nitrogen (fig. 8(c)). At $7,000^{\circ}$ K where nitrogen is 50 percent dissociated, the anomalous ultrasonic absorption is already three to four times as large as α_{class} . At $13,000^{\circ}$ K where nitrogen is 25 percent ionized, the anomalous absorption is almost an order of magnitude larger. Carnevale et al., in their discussion of the anomalous absorption coefficient, concluded that "Mechanisms such as dissociation and ionization reactions, and the excitation of electronic states appear to be frozen out of the sound wave at megahertz frequencies. If the above mechanisms are frozen out then the radiative heat transport would be responsible for the large sound absorptions at these elevated temperatures." It appears that these statements are conjectures, as no substantive arguments or calculations were included in reference 16. In the next few paragraphs of this paper two different arguments will be used to show why the anomalous ultrasonic absorption for nitrogen cannot be attributed to thermal radiation.

The first approach is to use estimated values of the spectral emission coefficients to calculate α_{rad} , then compare the sum of α_{rad} and α_{class} with the measured ultrasonic absorption coefficients of reference 16. However, there are uncertainties in the estimated spectral emission coefficients which could affect the values of α_{rad} by one to two orders of magnitude. Consequently, another approach is to take the anomalous ultrasonic absorption (i.e., difference between the measured and classical values) to calculate the corresponding radiative coefficient which is a measure of the spectral emission coefficients averaged over the entire spectrum of wavelengths. This radiative coefficient will then be examined to determine whether its temperature variation is reasonable.

The two approaches require the use of the expression relating the ultrasonic absorption coefficient, α_{rad} , to radiative quantities. This expression is obtained from the same linearized equations of motion that yield the expression for the classical absorption. In the derivation of α_{class} the radiative terms were discarded in order to effect a solution. In the derivation of α_{rad} the viscous and thermal conductive terms are discarded. The

resulting expression for the ultrasonic absorption induced by radiation³ is given in reference 17 as

$$\left(\frac{\alpha_{\text{rad}}}{k_0}\right)^2 = \frac{1}{2} \gamma \left[\frac{(1 + S'^2)^{1/2} (1 + \gamma^2 S'^2)^{1/2} - (1 + \gamma S'^2)}{1 + \gamma^2 S'^2} \right] \quad (27)$$

and the corresponding dispersion relation is given as

$$\left(\frac{c}{c_0}\right)^2 = \frac{2}{\gamma} \frac{1 + \gamma^2 S'^2}{(1 + S'^2)^{1/2} (1 + \gamma^2 S'^2)^{1/2} + (1 + \gamma S'^2)} \quad (28)$$

where γ is the ratio of specific heats and k_0 is the acoustic propagation constant, ω/c_0 . The quantity S' is the ratio

$$S' = \frac{\omega}{Q} \quad (29)$$

The quantity Q is the coefficient of proportionality in the expression for the divergence of the radiative heat flux vector

$$\frac{\partial}{\partial x_i} (q_i)_{\text{rad}} = \rho c_v Q (T - T_0) \quad (7)$$

Hunt calls this quantity the "radiation coefficient." The relationship between the radiation coefficient and the radiative absorption coefficient, $\mu(\lambda_r)$, was derived by Smith (ref. 30). This relationship is given as

$$Q = \frac{k_0}{\rho c_v} \int (h - h^2 \cot^{-1} h) \frac{\partial J_b}{\partial T} d\lambda_r \quad (30)$$

where h is the normalized radiative absorption coefficient

$$h(\lambda_r) = \frac{\mu(\lambda_r)}{k_0} \quad (31)$$

³From a mathematical viewpoint, the effect of thermal radiation on ultrasonic waves can actually be classified as a relaxation mechanism. This entire section will be devoted to a discussion of radiation due to its importance in high temperature energy transfer. Other relaxation mechanisms will be discussed in the next section.

and J_b is the black-body function per unit wavelength

$$J_b = 2ha^2\lambda_r^{-5} \left[\exp \left(\frac{ha}{\lambda_r kT} \right) - 1 \right]^{-1} \quad (32)$$

where h is Planck's constant and a is the speed of light.

The first approach in determining the importance of α_{rad} is to use relatively accurate values of Q to calculate α_{rad} , then compare the sum of α_{rad} and α_{class} with the measured ultrasonic absorption of reference 16. It is difficult to find radiative properties of nitrogen or argon⁴ in a convenient form. Therefore, the radiative emission coefficients of air from reference 31 will be used in this paper as a first approximation for those of nitrogen. Typical emission coefficients from reference 31 are shown in figure 9. A cursory inspection of the separate radiative absorption coefficients for the various constituents of air indicate that $\mu(\lambda_r)$ for nitrogen would be overestimated in these calculations by less than 20 percent for temperatures above 7,000° K. At temperatures below 5,000° K the radiative absorption coefficient for nitrogen may be overestimated in these calculations by as much as one or two orders of magnitude due to the presence of the Schumann-Runge radiation from molecular oxygen. This uncertainty due to the presence of oxygen is unimportant since α_{rad} is relatively small at these lower temperatures. At the higher temperatures Sewell's mean radiative absorption coefficients appear to be lower by factors of 3 to 8 when they are compared with those from more exact calculations (refs. 32 to 35). The largest portion of this discrepancy can be attributed to the use of incorrect cross sections in the vacuum ultraviolet. Consequently, the values of Q based on Sewell's spectral emission coefficients and equation (30) are increased by a factor of 10 before they are substituted into equation (27). The resulting values of Q are shown in figure 10. The quantity Q is relatively constant between 4,000° and 7,000° K because of the presence of the Schumann-Runge band, but increases quite rapidly at higher temperatures. The corresponding values of S' range from 10^6 at 6,000° K to 10^2 at 20,000° K. The values of α_{rad} for nitrogen, based on the radiative emission coefficients of figure 9, are shown in figure 11. At 4,000° K, α_{rad} is smaller than α_{class} by five orders of magnitude. Even at 20,000° K, α_{rad} is smaller by one order of magnitude. Consequently, these calculations have shown that thermal radiation cannot account for the anomalous ultrasonic absorption measured by Carnevale.

At present there are many uncertainties associated with the prediction of radiative quantities. Consequently, it would be useful to analyze the

⁴The effect of thermal radiation on ultrasonic absorption in argon will not be calculated. However, the conclusions based on an examination of nitrogen radiative properties should hold for argon as calculations and measurements in references 8 and 31 show that the magnitude of the total radiation from argon should be within a factor of two of that from nitrogen.

role of thermal radiation without relying on absolute values of the radiative emission coefficients. An alternate approach is to calculate the radiative coefficient, Q , corresponding to the anomalous ultrasonic absorption coefficient. This radiative coefficient will then be examined to determine whether its temperature variation is reasonable. Rather than solving equation (27) directly for S' , it is much easier to calculate values of α_{rad} for a range of values of Q for constant values of the sound speed and frequency of the ultrasonic wave (i.e., constant temperature and pressure). The results of this calculation are shown in figure 12. Two representative values of γ are used. The ordinate is the normalized ultrasonic absorption coefficient, α_{rad}/k_0 , where k_0 , the acoustic propagation constant, is defined as

$$k_0 = \omega/c_0 \quad (33)$$

Both k_0 and ω are assumed to be constants in this figure. The abscissa S' is inversely proportional to the radiation coefficient, Q (i.e., large values of S' correspond to low levels of thermal radiation). Typical values of S' for conditions corresponding to those in reference 16 vary from 10^6 to 10^2 . At low levels of thermal radiation, the ultrasonic absorption is small in this region, as one would expect from an analogy with the ultrasonic absorption due to heat conduction. At much higher levels of thermal radiation ($S' \ll 1$), the ultrasonic absorption falls off rapidly. This phenomenon can be explained as follows. As the radiative absorption coefficient increases beyond a certain level, the effective transmission of thermal radiation occurs in a distance which is much smaller than an acoustical wavelength. Consequently, the energy transfer over one acoustical wavelength is small. At intermediate values of thermal radiation ($S' \approx 1$), the peak value of α_{rad}/k_0 and the corresponding value of S' can be obtained from equation (27). These values are

$$\frac{\alpha_{\text{rad}_{\text{max}}}}{k_0} = \frac{\gamma - 1}{[8(\gamma + 1)]^{1/2}} \quad (34)$$

$$S'_{\text{critical}} = \frac{1}{\gamma} \left(\frac{3\gamma + 1}{\gamma + 3} \right)^{1/2} \quad (35)$$

Note that the peak value is independent of the radiation coefficient, although a specific value of the radiation coefficient is required to reach $\alpha_{\text{rad}_{\text{max}}}$.

The results of the calculations described in the last paragraph will now be used to determine the temperature variation of the radiation coefficient, Q . The first step is to compare the sum of $\alpha_{\text{rad}_{\text{max}}}$ and α_{class} for nitrogen with Carnevale's measured values (fig. 13). It can be seen that both the magnitudes and temperature variations compare quite well at temperatures above 6,000° K. The comparison also indicates that if the proper combination of c_0 , ω , and Q were to exist then it would be possible for thermal radiation to produce the anomalous ultrasonic absorption. Since the value of c_0 is known at each temperature, and the ultrasonic frequency is fixed at 1 Mc,

only one value of the radiation coefficient corresponds to $\alpha_{\text{rad max}}^5$. This quantity will be called $Q_{\text{max } \alpha}$. Its temperature variation, shown in figure 14 by a dashed curve, is normalized to the value at $6,000^\circ \text{ K}$. Figure 14 shows that $Q_{\text{max } \alpha}$ is relatively constant for temperatures as high as $20,000^\circ \text{ K}$. How does this value of Q compare with the more realistic values based on calculated radiative absorption coefficients of reference 31? These more realistic values are also shown in figure 14, normalized to the value at $6,000^\circ \text{ K}$. It can be seen that this radiation coefficient based on calculated radiative properties increases by four orders of magnitude⁶ as the temperature increases from $6,000^\circ$ to $20,000^\circ \text{ K}$ in contrast to the almost constant value of $Q_{\text{max } \alpha}$ which would be required to satisfy the radiation hypothesis. Consequently, the conclusion is reached again that the radiation hypothesis is incorrect.

ULTRASONIC ABSORPTION DUE TO RELAXATION EFFECTS

The effects of viscosity, thermal conductivity, and thermal radiation on ultrasonic absorption have been discussed in previous sections. These effects cannot account for the large absorption measured by Carnevale in nitrogen at temperatures above $6,000^\circ \text{ K}$, and in argon at temperatures above $10,000^\circ \text{ K}$. This leaves a variety of causes which can be grouped under the category of "relaxation phenomena." These phenomena include relaxation caused by population of vibrational and rotational molecular modes, by diffusion of chemical species, by chemical reaction rates, and by transitions of excited atomic states. Carnevale calculated the effects of rotational and vibrational relaxation and relaxation due to diffusion of chemical species (ref. 16) and found these effects to be relatively small above $6,000^\circ \text{ K}$. As for dissociation, and ionization relaxation, he stated that "Mechanisms such as dissociation and ionization reactions and the excitation of electronic states appear to be frozen out of the sound wave at megahertz frequencies."

Carnevale's calculations contain an inconsistency in that he included the effects of dissociation and ionization relaxation in calculating the speed of sound, but not in calculating the absorption coefficient. Comparison of these "frozen" sound speeds with the equilibrium sound speed shows differences as large as 25 percent. This comparison coupled with the fact that large amounts of relaxation energies are involved indicates that relaxation absorption in high-temperature nitrogen and argon should be examined more carefully.

⁵Although the magnitude of $\alpha_{\text{rad max}}$ is independent of Q , its attainment depends upon Q for a given c_0 and ω .

⁶It was mentioned earlier that Sewell's radiative emission coefficients (ref. 31) are in error because he underestimated the vacuum ultraviolet contribution. The data of reference 36 showing the contribution of vacuum ultraviolet radiation with increasing temperature indicate that the Q increase with temperature should even be larger than shown in figure 12, possibly as large as five or six orders of magnitude as the temperature is increased from $6,000^\circ$ to $20,000^\circ \text{ K}$.

When the ultrasonic frequency is much higher than the characteristic relaxation frequency, the question arises as to whether it is valid to assume that the relaxation absorption is negligible. This question may be answered by comparing the frequency dependence of relaxation absorption with the frequency dependence of classical absorption. Typical frequency variations of the absorption coefficient α , and the absorption coefficient per wavelength,⁷ $\alpha\lambda_s$, are shown in figure 15 for classical and typical relaxation absorption (ref. 10). The quantity α_{class} varies essentially as f^2 , whereas the quantity $\alpha_{\text{class}}\lambda$ varies as f (eq. (18)). In contrast, the quantity α_{relax} has a very low value at frequencies below the resonance or characteristic frequency of the relaxation phenomenon.⁸ In the vicinity of this resonance frequency the curve would experience a sudden increase, finally leveling off. At frequencies much higher than the resonance frequency, α_{relax} is a constant. This variation is also shown in figure 16 for a large range of relaxation times. The numerical values are typical of those for vibrational relaxation, but the trends are typical of any relaxation phenomenon. In figure 15 the curve of frequency versus $\alpha_{\text{relax}}\lambda_s$ has the shape of a Gaussian distribution curve.

Unfortunately, the literature is inconsistent in the use of the word "absorption." Some authors use this term to describe α , whereas others use it to describe $\alpha\lambda_s$. In the latter case the statement is sometimes made that the relaxation "absorption" approaches zero as the frequency increases beyond the characteristic frequency (fig. 15). Apparently, Carnevale used this as a criterion for neglecting dissociative and ionization relaxation in high-temperature nitrogen.

The different behavior of the classical and relaxation absorption as the frequency is changed results in one absorption mechanism predominating in a given frequency range and the other predominating in another frequency range. If the characteristic relaxation time were sufficiently low and the energy for that mechanism were sufficiently high, the relaxation absorption could be extremely large as shown in figure 16. In fact, experimental data (ref. 37) indicate that relaxation absorption can be as much as 10 to 20 times larger than classical absorption at the resonance frequency. On the other hand, the shapes in the frequency variations in figure 15 show that if the frequency is sufficiently higher than the resonance frequency, then α_{class} would be much higher than α_{relax} . The question is what constitutes "sufficiency?" Obviously, the criterion would depend on two parameters. The first is the ratio $\alpha_{\text{relax}}/\alpha_{\text{class}}$ at the resonance frequency, and the second is the half width of the $\alpha_{\text{relax}}\lambda_s$ versus f curve. Neither α_{class} nor α_{relax} appears to have a theoretical limit. As a result, there are no upper or lower bounds for the ratio $\alpha_{\text{relax}}/\alpha_{\text{class}}$ for a given relaxation process. Furthermore,

⁷The term "absorption coefficient per wavelength" is a misnomer; it actually refers to the product of the absorption coefficient and the ultrasonic wavelength.

⁸For example, the characteristic vibrational frequency is 2π times the reciprocal of the vibrational relaxational time.

there is no simple expression for $\alpha_{\text{relax}}/\alpha_{\text{class}}$ as a function of the frequency. This means that for a given situation (i.e., temperature, pressure, and ultrasonic frequency), the various α_{relax} must be calculated and compared with α_{class} to determine if each α_{relax} is negligible.

Chemical relaxation will be examined first. This relaxation occurs when the chemical reaction times are long compared with an ultrasonic period, thereby preventing the attainment of chemical equilibrium. The theory used in this paper was derived by Damköhler in reference 38 and was chosen because of its generality. For example, it accounts for several simultaneous chemical reactions, and it is not restricted to the dissociation process. It was also chosen because of its convenient form, since it directly relates the reaction rate coefficients with ultrasonic absorption.

Damköhler assumes that the ultrasonic-induced compression and expansion in the gas are, to a first approximation, isentropic. The isentrope is represented by the general polytropic equation

$$pV^m = \text{constant} \quad (36)$$

where the isentropic exponent, m , is a function of the chemical composition, the ultrasonic frequency, and the chemical reaction rate. In the limit of a nonreactive gas and zero frequency, m is identical with γ , the ratio of specific heats. From equation (36) it follows that

$$\frac{\delta p}{p} + m \frac{\delta V}{V} = 0 \quad (37)$$

Damköhler then uses the mass conservation equation, the momentum conservation equation, and the energy conservation equation⁹ (first law of thermodynamics). All state variables (p , T , V , ρ , N) are assumed to vary sinusoidally about a mean value (p_0 , T_0 , V_0 , ρ_0 , N_0). For example, the pressure variation is

$$p = p_0 + \delta p + \text{Re}[\underline{p} \exp(gx + ht)] \quad (38)$$

where the underlined letter designates a complex quantity which takes into account the phase angle between the various quantities. Up to this point the derivation is similar to that for classical absorption. Damköhler's major contribution is the relation between the forward and reverse reaction rates and the differential changes δp , δT , and δn_i . The final expression relates the reaction rate at equilibrium with m , the polytropic exponent, and φ the phase angle between the pressure change and the density change. This expression for the special case of a single chemical reaction (designated by the subscript "1") is given in the determinant form

⁹Damköhler drops the viscosity term in the momentum equation and the thermal conductivity, radiation, and diffusion terms in the energy equation.

$$m \exp(i\phi) = \gamma + \frac{\begin{vmatrix} 0 & A_1 \\ A_1 & B_{11} + i\phi_{11} \end{vmatrix}}{\begin{vmatrix} 1 & A_1 \\ C_1 & B_{11} + i\phi_{11} \end{vmatrix}} \quad (39)$$

The quantities A_1 , B_{11} , C_1 , and ϕ_{11} are defined as follows:

$$A_1 = \gamma v_1 - (\gamma - 1) \frac{W_1}{RT} \quad (40)$$

$$B_{11} = \frac{W_1 v_1}{RT} + \sum_j v_{j1}^2 \frac{n_j}{n_1} - v_1^2 \quad (41)$$

$$C_1 = \frac{W_1}{RT} - v_1 \quad (42)$$

$$\phi_{11} = \frac{2\pi f N}{U_1 V} \quad (43)$$

where W_1 is the heat of reaction, v_{j1} the stoichiometric coefficient for the j th molecule, v_1 the sum of the stoichiometric coefficients, N the total number of mols, and U , the reaction rate at equilibrium. Equations (39) through (43) show that both m and ϕ are functions of the ultrasonic frequency and the reaction rate. The relation between m and ϕ on one hand and the ultrasonic absorption and dispersion due to chemical relaxation on the other hand are

$$c = \sqrt{\frac{mRT}{\bar{M}}} \frac{1}{\cos(\phi/2)} \quad (44)$$

$$\alpha_{\text{react}} = 2\pi f \sqrt{\frac{\bar{M}}{mRT}} \sin \frac{\phi}{2} \quad (45)$$

where \bar{M} is the mean molecular weight of the reactive gas. The expression for the ultrasonic absorption, α_{react} , in equations (39) and (45) is very complex, in comparison to the comparable expression for vibrational relaxation (ref. 9).

Dissociative relaxation in nitrogen will be discussed first. The measurement of dissociation rates may be obtained by two different types of

experiment. The first utilizes a small perturbation (e.g., an ultrasonic wave) to form regions slightly out of equilibrium. The second utilizes a large disturbance (e.g., flash photolysis or a shock wave) to create a distinct zone far from equilibrium. The dissociation rate constants from the two different types of experiment may not necessarily be the same. Pritchard (ref. 39) discussed the effects of anharmonicity on the dissociation of molecules. In particular he examined the variation of $N_{i,i+1}$, the number of molecules per second making a transition from a state i to the neighboring state $i + 1$, as i varies from the ground vibrational state to the continuum. Pritchard observes that $N_{i,i+1}$ may have a minimum. From this behavior, he concludes that for the special case of a diatomic molecule, the forward rate coefficient measured by the shock wave or flash photolysis technique is lower than the equilibrium forward rate coefficient (i.e., the rate coefficient measured by the ultrasonic technique). Consequently, if an accurate estimation of α_{diss} is required, then values of k_d must be determined by near-equilibrium techniques. Unfortunately, these values are not available. The only alternative is to use the few available shock tube measurements of k_d . The resulting values of α_{diss} would be lower by an undetermined amount than those obtained in an actual ultrasonic experiment.

Very few measurements of the nitrogen dissociative rate coefficients are available. Recent measurements were reported by Byron (ref. 40) for pure nitrogen and for a series of argon-nitrogen mixtures. Allen, Keck, and Camm (ref. 41) also made measurements in pure nitrogen. Byron measured dissociation rate coefficients by using interferometric measurements of the change in gas density behind shock waves. The rate coefficients for $N_2 - N_2$ collisions and $N_2 - N$ collisions in units of $\text{cm}^3/\text{mol}/\text{sec}$ are

$$k_{d_{N_2-N_2}} = 4.8 \times 10^{17} T^{-1/2} \exp\left(-\frac{E_d}{RT}\right) \quad (46)$$

$$k_{d_{N_2-N}} = 4.3 \times 10^{22} T^{-3/2} \exp\left(-\frac{E_d}{RT}\right) \quad (47)$$

where the dissociation energy, E_d/R , has the value $113,200^\circ \text{K}$. The magnitude of the forward reaction rate, U_1 , is related to these rate coefficients by

$$U_1 = k_{d_{N_2-N_2}} [N_2][N_2] + k_{d_{N_2-N}} [N_2][N] \quad (48)$$

where $[N_2]$ and $[N]$ are mol concentrations of molecular and atomic nitrogen. For large degrees of dissociation the second term on the right in equation (48) is the predominant one and will determine the peak value of α_{diss} since the rate constant for $N_2 - N$ collisions is an order of magnitude larger than that for $N_2 - N_2$ collisions and since $[N_2][N_2] \ll [N_2][N]$ in the temperature range of interest.

Before the rate coefficients given in equations (46) and (47) are used to calculate α_{diss} , it should be determined whether their range of validity

covers the conditions of Carnevale's ultrasonic experiments. These conditions are: (1) temperatures ranging from 6,000° to 10,000° K, and (2) the amount of dissociation ranging from 10 to 100 percent. Byron stated that "Temperatures from 6,000° K to 9,000° K were covered in the experiments." This is the range of validity for the $A - N_2$ forward rate and, to a lesser degree, the range of validity for the $N_2 - N_2$ forward rate coefficients. However, this does not mean that the $N_2 - N$ forward rate coefficients in equation (47) are valid throughout this temperature range. The major portion of the data which was used to infer the $N_2 - N$ rate coefficients came from the runs using pure nitrogen. In these runs the maximum amount of dissociation was only in the neighborhood of 5 percent. This small amount of dissociation results in several disadvantages. First, the effects of $N_2 - N$ collisions on the dissociation rate would be, at most, the same order of magnitude as the effects of $N_2 - N_2$ collisions. Since Byron's data determine the sum of the two effects, an accurate separation of the $k_{d_{N_2-N}}$ term is exceedingly difficult. Second, the effects of $N_2 - N$ collisions are only evident when equilibrium conditions are approached (i.e., for temperatures slightly greater than the equilibrium temperature. Calculations show that these equilibrium temperatures are no higher than 5400° K. Because of these disadvantages, the magnitude and temperature variation of the $N_2 - N$ forward rate coefficients (eq. (47)) is in doubt for temperatures higher than 6,000° K.

The experiment of Allen, Keck, and Camm was performed with a different diagnostic technique - the monitoring of optical radiation from the $N_2(1+)$ band system. Dissociation rates behind shock waves can be studied because of the short radiative and vibrational relaxation times. This experiment is superior to Byron's experiments in two respects. First, a combustion drive shock tube is used instead of a conventional cold drive shock tube. This results in higher equilibrium temperatures (6,800° K) and higher degrees of dissociation (50 percent). Second, the measurement of the $N_2 - N$ rate coefficient is essentially independent of the measurement of the $N_2 - N_2$ rate coefficient. Unfortunately, the temperature range of the experiment was limited so that a single value of the $N_2 - N$ rate coefficient was obtained (2.8×10^9 cm³/mol/sec at 6,400° K). The temperature variation could not be determined from the limited data.

For the calculations of α_{diss} in this paper, it was decided to use Byron's expression for the $N_2 - N_2$ rate coefficient (eq. (46)), and to multiply Byron's expression for the $N_2 - N$ rate coefficient by a factor of 1.38 so that his value would coincide with Allen's value at 6,400° K. The resulting values of α_{diss} are compared in figure 17 with those for α_{class} and Carnevale's measured values of the total absorption. The values of α_{diss} peak quite sharply at 50-percent dissociation (7,500° K). Some observations can be made on the values of α_{diss} in the vicinity of this peak. First, the $N_2 - N$ contribution to α_{diss} is 15 times the $N_2 - N_2$ contribution. This points out the fact that if a measurement of α_{diss} at large degrees of dissociation is possible, then it is essentially a measurement of the $N_2 - N$ rate coefficients. Second, the use of rate constants which are surmised to be lower than those existing in Carnevale's experiments results in values of

α_{diss} which are not negligible. The peak value of α_{diss} is 40 percent of α_{class} . But these values of α_{diss} are still too low (by a factor of 8) to account for the anomalous absorption at 7,500° K. It is debatable whether the difference between the equilibrium values of k_d and those measured by shock-wave techniques can account entirely for the anomalous absorption. One final observation can be made. For the sake of argument, assume that the values of k_d are sufficiently large that the sum of α_{diss} , α_{vib} , and α_{class} matches Carnevale's experimental values at 7,500° K. The comparison over the entire temperature range is shown in figure 18. The theoretical values compare quite well for temperatures up to 7,500° K. However, from 7,500° K to 10,000° K¹⁰ the theoretical values decrease rapidly, whereas the experimental values remain essentially constant. There may be several different explanations for this apparent anomaly. One possible explanation is that the additional absorption in the vicinity of 10,000° K indicates the presence of extraneous experimental effects such as large temperature gradients in the plasma, which are inherent characteristics of plasma arcs, or the additional absorption may be attributed to the large thermal boundary layers on the faces of the ultrasonic transducer and receiver. A second possible explanation is that the equilibrium values of k_d are not much larger than the shock wave measured values after-all, and that a large part of the anomalous absorption in nitrogen can be attributed to another relaxation phenomenon whose effect remains relatively constant as the temperature increases. This relaxation phenomenon due to collisional excitation of bound electrons will be discussed in the section following the discussion on ionization relaxation.

Ionization relaxation may be an important factor in Carnevale's experiment at temperatures greater than 10,000° K for both nitrogen and argon. Damköhler's derivation of the absorption due to reactive relaxation is so general that it can be applied to the ionization case as well as the dissociative case. Therefore, equations (36) through (45) can be used directly. However, the forward reaction rate is now given by

$$U_1 = k_{i_{A-A}}[A][A] + k_{i_{A-A^+}}[A][A^+] + k_{i_{A-e}}[A][e] \quad (49)$$

where $[A]$, $[A^+]$, and $[e]$ are mol concentrations of the atom, ion, and electron. The ionization rate constants have usually been calculated from measured excitation or ionization cross sections (refs. 42 and 43). Of these, only the rate constants for argon have been studied experimentally. Petschek and Byron (ref. 5) measured forward rates behind shock waves by making use of (1) the visible continuum radiation from the gas, and (2) the electrostatic potentials in the gas due to the diffusion of electrons. They found that in the final stage of ionization, where the conditions approach those found in an ultrasonic pulse, the electron-atom rate coefficient is accurate. Petschek and Byron also concluded that the reaction rate for argon is completely

¹⁰Beyond 10,000° K there is another rise in the absorption due to ionization relaxation. This phenomenon will be discussed in the next section. However, this absorption should be negligible between 7,500° K and 10,000° K because of the small number density of electrons.

dominated by electron-atom collisions. For these reasons, α_{ion} in argon can be calculated with a fair amount of confidence.

The ionization process due to electron-atom collisions is described as a two-step process by Petschek and Byron. The first step is an inelastic collision between a free electron and a ground state argon atom, where the atom receives sufficient energy to raise one of its bound electrons into the first excited state.



Quantum mechanical selection rules show that this state is a metastable state. The lifetime of this metastable state is much larger than the collision time, thereby allowing a second inelastic collision with another free electron which produces ionization of the bound electron.



The rate coefficient used by Petschek and Byron is based on the inelastic cross section measurements by Maier-Leibnitz (ref. 42). The expression for the rate coefficient, in units of $\text{cm}^3/\text{mol}/\text{sec}$, is

$$k_{iA-e} = 2.16 \times 10^8 T^{3/2} \left(\frac{E_e}{RT} + 2 \right) \exp \left(- \frac{E_e}{RT} \right) \quad (52)$$

where the value of $134,000^\circ \text{K}$ was used for the excitation energy, E_e/R . The ionization process due to ion-atom collisions is much less effective than the process due to electron-atom collisions. A qualitative comparison of the appropriate cross sections (refs. 44 and 45) and velocities indicates that the ratio of the ion-atom rate constant to the electron-atom rate constant is extremely small. Since the product $[A][A^+]$ is equal to the product $[A][e]$ in equation (49), the ratio of the second term to the third term on the RHS of equation (49) is also extremely small. As a result, the ion-atom effects can be neglected. The atom-atom term in equation (49) becomes dominant only at ionization levels below 10^{-3} . But at these levels α_{ion} is negligible.

However, the atom-atom rate constant deserves mention for two reasons. First, the mechanism described by Harwell and Jahn (ref. 46) is assumed to be similar to the two-step mechanism described for the electron-atom ionization process. The only difference is that the free electron is replaced by a ground state atom. Second, Harwell and Jahn verified this mechanism in an experiment described in reference 47. They showed that the excitation step is rate controlling and that it has an activation energy approximately equal to the energy of the first excited state. This experimental verification is important in that it is an additional (although indirect) verification of the dominant two-step mechanism proposed for the electron collisions. The atom-atom coefficient given by Appleton (ref. 47) is

$$k_{iA-A} = 1.38 \times 10^{12} \exp \left(- \frac{E_e}{RT} \right) \quad (53)$$

A comparison of the values from equations (52) and (53) shows that the atom-electron rate coefficient is roughly 1000 times greater than the atom-atom rate coefficient over the temperature range where single ionization is important.

These rate coefficients were used to calculate α_{ion} for argon. The results are presented as the sum of α_{ion} and α_{class} in figure 19 along with Carnevale's measured values. The values of α_{ion} become perceptible at 1-percent ionization. The peak value is reached near 50 percent ionization which is characteristic of relaxation due to incomplete chemical reactions, but does not drop off as sharply as the absorption due to dissociation. The peak value of α_{ion} is 13 times as large as α_{class} . The calculated value of $\alpha_{ion} + \alpha_{class}$ passes through the middle of the experimental points. In addition, both the calculated and measured values show the same initial increase in absorption at 10,000° K and show roughly the same rate of decrease as the temperature increases from 15,000° to 20,000° K. An unqualified statement that ionization relaxation can account for the anomalous ultrasonic absorption in argon cannot be made because of the large scatter in the experimental data. If the elimination of the scatter were not possible, a change in the gas pressure might be another means of verification. For example, an increase of pressure from 1 to 10 atmospheres should have two effects. The first is to move the absorption peak from 14,500° to 17,200° K, and the second is to increase α_{ion} by a factor of 5 due to an increase of 5 in the electron-atom rate coefficient (eq. (52)) which depends only upon temperature.

A calculation of α_{ion} in nitrogen cannot be performed with the same degree of confidence because the ionization rate constants for nitrogen have not been verified experimentally. Bortner (ref. 48) presented theoretical values of the atom-atom and atom-electron rate coefficients. He assumed a single step process for both types of collisions. The values quoted in reference 48 are

$$k_{iN-e} = 2.7 \times 10^{13} T^{1/2} \exp\left(-\frac{E_i}{RT}\right) \quad (54)$$

$$k_{iN-N} = 6.0 \times 10^4 T^{3/2} \exp\left(-\frac{E_i}{RT}\right) \quad (55)$$

where the ionization energy, E_i/R , has the value 168,750° K. Note that the pre-exponential factor in the atom-electron rate constants for argon (eq. (52)) and nitrogen (eq. (54)) are roughly the same. The difference in the two rate constants is in the values used for the activation energy (excitation energy of 134,013° K for argon, and ionization energy of 168,750° K for nitrogen). This results in a much lower value of α_{ion} in nitrogen.

The rate constants in equations (54) and (55) were used to calculate α_{ion} for nitrogen. The results are presented as the sum of α_{ion} and α_{class}

in figure 20. Carnevale's measured values are also shown. At 10,000° K where the degree of ionization is low, α_{ion} is negligible, so that the total calculated absorption is 6 times smaller than the experimental values. The peak value of α_{ion} is reached at 14,500° K and is roughly twice the value of α_{class} . Based on the rate coefficients in equations (46), (47), (54), and (55) it appears that dissociative and ionization relaxation cannot account for the bulk of the anomalous absorption in nitrogen.

The statement was made earlier that the anomalous ultrasonic absorption in nitrogen also existed when the nitrogen particles were predominantly in the atomic form. This indicates that the anomalous absorption at this condition may be attributed to the relaxation phenomenon associated with the electronic structure of the atom. It is also possible that this phenomenon accounts for the bulk of the anomalous absorption in nitrogen over the entire temperature range above 6000° K, since a sizable fraction of the particles are in the atomic form (fig. 21). The following approach will be used to determine if such a relaxation phenomenon exists. First, the anomalous absorption of argon and nitrogen will be compared at conditions where the gas particles are predominantly in the atomic form. Then an attempt will be made to explain the differences in the anomalous absorption for the two gases in terms of their atomic properties. The last step is to make an order of magnitude calculation to determine if the characteristic relaxation time for electronic excitation (i.e., inelastic cross section) required for the anomalous absorption can be attained.

The comparison will be made at a temperature of 10,000° K and a pressure of 1 atmosphere, where the equilibrium composition of the two gases is shown in the following table:

	$n_{molecule}$	n_{atom}	$n_{ion} \approx n_{electron}$
Nitrogen	0.03×10^{17}	6.95×10^{17}	0.18×10^{17}
Argon	0	7.04×10^{17}	0.15×10^{17}

Note that the number densities of nitrogen and argon atoms are approximately the same. The relative lack of molecules and ions indicates that reactive relaxation is not a factor at this condition. Figure 8(c) shows that the anomalous absorption for nitrogen is 6 times the classical value, whereas figure 8(a) shows very little anomalous absorption for argon. Consequently, if the anomalous absorption is associated with a particular process in the nitrogen atom, the same process must occur to a much lesser degree in the argon atom. The next step is to compare certain atomic parameters for nitrogen with those for argon. These parameters are the energy level of the first excited state (ref. 49) ϵ_1/k , and the parameter $g_1 \exp[-(\epsilon_1/kT)]$, where g_1 is the statistical weight of the first excited state. This last parameter is proportional to the collisional probabilities of the state, and the specific heat associated with the state is a complex function of the two parameters (eq. (58)). The values of these parameters are

	$\epsilon_1/k,$ $^{\circ}\text{K}$	$g_1 \exp(-\epsilon_1/kT)$ ($T = 10,000^{\circ}\text{K}$)
Nitrogen atom	27,656	0.629
Nitrogen ion ^a	22,031	0.552
Argon atom	134,420	1.16×10^{-5}
Argon ion ^a	156,391	4.84×10^{-7}

^aThe parameters for the nitrogen and argon ions are included for use in a later discussion.

The comparison of ϵ_1/k shows that the first excited state of the nitrogen atom is much lower than that for the argon atom. The comparison of values for $g_1 \exp(-\epsilon_1/kT)$ shows that collisional formation of the first excited level for nitrogen atoms is much more probable. Since the atom-atom collision cross sections for argon and nitrogen are comparable, then the relaxation time for the formation of the first excited level for nitrogen atoms should also be lower. Substitution of the values of ϵ_1/kT and $g_1 \exp(-\epsilon_1/kT)$ into the expressions for the specific heat associated with this excited state (eq. (58)) also shows a much larger value for nitrogen. Since the absorption due to relaxation is proportional to the specific heat and inversely proportional to the relaxation time (eq. (56)), then the absorption attributed to the finite time required for the collisional formation of the first excited state will be much larger in nitrogen than it will be in argon. This contrast in absorption in the two gases seems to agree with that observed in Carnevale's experimental values at $10,000^{\circ}\text{K}$.

This supposition of collisional relaxation in nitrogen can be partially substantiated by an order of magnitude calculation to determine if the characteristic relaxation time can be realized physically. The problem can be vastly simplified if it is assumed that collisional excitation occurs only for one given transition (i.e., if the process can be defined by a single relaxation time). It will be shown in the next paragraph that this assumption is a fairly good one for nitrogen atoms. Once the single step relaxation is assumed, the ultrasonic absorption can be related to the specific heats and relaxation time by

$$\alpha_{\text{exc}} = \frac{\omega}{2c(\omega)} \frac{\omega \tau_{\text{exc}} R c_{v_{\text{exc}}}}{(R + c_{v_0}) c_{v_0} + \omega^2 \tau_{\text{exc}}^2 (R + c_{v_{\infty}}) c_{v_{\infty}}} \quad (56)$$

The derivation of this equation can be found in reference 50. The speed of sound in equation (56) can be obtained from

$$c^2(\omega) = \left(\frac{\partial p}{\partial \rho} \right)_T \frac{(R + c_{v_0}) c_{v_0} + \omega^2 \tau_{\text{exc}}^2 (R + c_{v_{\infty}}) c_{v_{\infty}}}{c_{v_0}^2 + \omega^2 \tau_{\text{exc}}^2 c_{v_{\infty}}^2} \quad (57)$$

No experimental or theoretical values of the excitation cross sections are available. Consequently, the approach is to assume a range of values of τ_{exc} , in order to determine if any of the resulting values for α_{exc} are as large as those for the anomalous absorption in nitrogen. The first step is to determine the equilibrium specific heat, c_{v_0} , and the specific heat due to electronic excitation, $c_{v_{\text{exc}}}$. If a Boltzmann distribution of states is assumed (ref. 51), the expression for the specific heat is

$$\frac{c_{v_0}}{R} = \frac{3}{2} + \frac{\sum \left(\frac{\epsilon_n}{kT} \right)^2 g_n e^{-\frac{\epsilon_n}{kT}}}{\sum g_n e^{-\frac{\epsilon_n}{kT}}} - \left(\frac{\sum \frac{\epsilon_n}{kT} g_n e^{-\frac{\epsilon_n}{kT}}}{\sum g_n e^{-\frac{\epsilon_n}{kT}}} \right)^2 \quad (58)$$

The values of g_i and ϵ_i were obtained from reference 49. The table below shows the effect of terminating the sums in equation (58) at different electronic states.

ATOMIC PROPERTIES OF ATOMIC NITROGEN AT $T = 10,000^\circ \text{ K}$.

Spectroscopic designation	Energy, ϵ_i cm^{-1}	$\exp - \frac{\epsilon_i}{kT}$	$\frac{c_{v_0}}{R}$	$\frac{\Delta c_{v_{\text{exc}}}}{R}$
$2p^3 \quad {}^4S^o$	0	1.000	1.500	0
$2p^3 \quad {}^2D^o$	19,226	.0629	2.400	.900
$2p^3 \quad {}^2P^o$	28,840	.0158	2.661	.261
$12d \quad {}^2D$	1116,625	4.69×10^{-8}	2.671	.010

The last column represents the difference between adjacent states. It can be seen that the largest portion of the excitation specific heat can be attributed to transitions between the ground state and the first excited state. The additional excitation specific heat due to transitions to the second excited state is small but not negligible. However, the corresponding relaxation time, which is inversely proportional to $\exp(-\epsilon_i/kT)$, will be larger for the second excited state than for the first excited state as shown in the table above. Since α_{exc} is proportional to $c_{v_{\text{exc}}}/\tau_{\text{exc}}$ at sufficiently high frequencies (eq. (56)), then α_{exc} for the second excited state is an order of magnitude smaller than that for the first excited state.¹¹ Similarly,

¹¹The relaxation coupling between the two excited states is assumed negligible.

it can be shown that α_{relax} for the higher states is also negligible. Therefore, the assumption of a single relaxation process between the ground and first excited states is a fairly good one for an order-of-magnitude calculation.

The results of the calculation for atomic nitrogen at 10,000⁰ K as shown in figure 22 has a Gaussian-like distribution which peaks at 2.35×10^{-7} second. The maximum value of α_{exc} is almost four times as large as α_{class} . The sum of the excitation absorption and the classical absorption is 1.15 cm^{-1} , as compared to Carnevale's measured value of 1.6 cm^{-1} . Consequently, the atom-atom collisional excitation process can account for a large portion of the anomalous absorption, provided the collisional excitation times are within a certain range. The next step is to use simple kinetic theory to determine if this range of excitation times is reasonable.

The excitation time is not always the best criterion as to the reasonableness of a given transition since it is dependent upon the transition energy and the collision cross section. These last two parameters vary widely from one type of collision to another. A better criterion is the steric factor, P , the fraction of sufficiently energetic collisions that actually result in a transition or reaction (ref. 52). It is obvious that if the calculated steric factor is greater than unity, the corresponding excitation time would be unrealistic. The steric factor is related to the excitation time by

$$\tau_{\text{exc}} = z_{\text{trans}}^{-1} = (z_{\text{elast}} \cdot f_{\epsilon} \cdot P)^{-1} \quad (59)$$

where z_{trans} is the rate at which a single atom undergoes a transition or reaction, and z_{elast} is the rate of collision of a single atom with other atoms, based on elastic scattering cross section. The quantity f_{ϵ} is the fraction of collisions in which the relative translational energy along the line of centers exceeds the excitation energy. The derivation of f_{ϵ} can be found in reference 52, and is given as

$$f_{\epsilon} = \exp\left(-\frac{\epsilon_{\text{exc}}}{kT}\right) \quad (60)$$

The excitation time corresponding to the peak value of α_{exc} and the elastic scattering cross section from reference 29 were used to calculate the steric factor. The calculations contained the following numerical values:

$$\tau_{\text{exc}} = 2.35 \times 10^{-7} \text{ sec}^{-1}$$

$$\pi 0^2 \Omega^{(2.2)*} = 1.13 \times 10^{-15} \text{ cm}^2$$

$$n = 7.34 \times 10^{17} \text{ cm}^{-3}$$

$$z_{\text{elast}} = 5.0 \times 10^8 \text{ sec}^{-1}$$

$$f_{\epsilon} = 0.0629$$

$$P = 0.135 = \frac{1}{7.4}$$

The times corresponding to z_{elast} and $z_{\text{elast}} \times f_{\epsilon}$ (i.e., $P = 1$) are shown in figure 22. Since the steric factor is less than unity, the corresponding excitation time can be realized physically. However, this does not positively identify collisional excitation as the source of anomalous absorption in nitrogen, since measured values of the excitation steric factor for other reactions range from slightly less than 1 to as low as 10^{-3} (refs. 44 and 45). It would be exceedingly difficult to verify directly the magnitude of the excitation cross section by a quantum-mechanical calculation because of the complexity of the situation. Equally as difficult would be a cross-beam experiment because of the extremely small spectral intensity emitted by the excited atoms. However, it may be possible to verify the importance of collisional excitation by an absorption measurement in some other gas, where the effect of collisional excitation is much easier to detect. The feasibility of this measurement will be discussed in a subsequent section.

For the sake of discussion, assume that collisional excitation of bound electrons is the source of anomalous absorption in atomic nitrogen. Then, it may be of interest to estimate the temperature variation of α_{exc} over a range of temperatures centered about $10,000^{\circ} \text{ K}$. The estimate accounts for the temperature dependence of the collision cross section, the excitation specific heat, and the energy cutoff factor, f_{ϵ} . The steric factor of $1/7.4$ is assumed to be constant over the temperature range. The effect of decreasing number density of nitrogen atoms is accounted for by multiplying the calculated value of α_{exc} by the mol fraction of atoms in the mixture. The result is shown in figure 23. This estimate should give a fairly good qualitative picture at temperatures less than $10,000^{\circ} \text{ K}$. However, at temperatures in excess of $10,000^{\circ} \text{ K}$, the values of α_{exc} shown in figure 23 are the lower limit, since there may be two additional sources of ultrasonic absorption due to collisional excitation. One of these stems from the collision of a nitrogen atom in the ground state with a free electron, where the transition is to be first excited state. The increasing importance of this particular transition with increasing temperature can be attributed to the rapid growth in the number of free electrons as shown in figure 21, and also to the fact that free electrons are more

efficient suppliers of excitation energy (ref. 53). Another source of ultrasonic absorption is the collisional excitation of the bound electron in the nitrogen ion, from the ground state ($2p^2\ ^3P$) to the first excited state ($2p^2\ ^1D$). It is possible that this class of transitions can result in as large a value of α_{exc} as that for the atom-atom collision. This is indicated by the table on page 30 and the following table which compares some of the pertinent parameters.

Transition	Temperature, °K	$\frac{\Delta c_{v_{\text{exc}}}}{R}$	f_{ϵ}	Collision partners	$\pi\sigma^2\Omega^{(2.2)*},$ cm ²
Nitrogen atom $2p^3\ ^4S^o \rightarrow 2p^3\ ^2D^o$	10,000	0.900	0.0629	N-N	1.13×10^{-15}
Nitrogen ion $2p^2\ ^3P \rightarrow 2p^2\ ^1D$	15,000	.217	.2302	N-N ⁺ e-N ⁺ N ⁺ -N ⁺	1.82×10^{-15} 5.2×10^{-14} 5.2×10^{-14}

The collisional transition for the nitrogen atom will be referred to as "case I" and the collisional transitions for the nitrogen ion as "case II." For large values of $\omega\tau_{\text{exc}}$,

$$\alpha_{\text{exc}} \sim \left(\frac{\Delta c_{v_{\text{exc}}}}{R} \right) (f_{\epsilon}) \left(\pi\sigma^2\Omega^{(2.2)*} \right) (P) \quad (61)$$

The table shows that the product of the first three factors on the right in equation (61) is smaller in case I. Unfortunately, numerical values for the excitation steric factors in both cases are not known, so that a direct comparison of α_{exc} for the two cases cannot be made. However, a qualitative comparison of certain parameters such as the strength of the interaction between collision partners and the distance of closest approach indicates that some of the excitation collisions in case II would have larger steric factors than the one in case I. It is therefore possible that the magnitude of α_{exc} at temperatures greater than 10,000° K would not fall as rapidly as shown in figure 23.

ABSORPTION MEASUREMENTS IN OTHER GASES

Earlier, the statement was made that it may be possible to verify the importance of collisional excitation by an absorption measurement in some other gas. Nitrogen has the disadvantage that it exists in a predominantly atomic form over an extremely narrow range of temperatures (fig. 21). As a result a temperature variation of α_{exc} due to atom-atom collisions cannot be accurately determined because of the rapid depletion of the atoms, the

presence of different collision partners, and because of other sources of ultrasonic absorption such as vibrational, dissociative, and ionization relaxation. Consequently, the alternate gas must have the restriction that it remain predominantly in the atomic form over a wider range of temperatures. Then appreciable absorption can arise from only three sources: (1) viscosity and thermal conductivity (i.e., classical absorption) due to atom-atom collisions, (2) collisional excitation of bound electrons by atom-atom collisions, and (3) thermal radiation from molecular, atomic, and charged particles. In addition, the measured ultrasonic absorption for this gas must be appreciably greater than α_{class} over a large portion of this temperature range. Oxygen between $6,000^{\circ}\text{K}$ and $10,000^{\circ}\text{K}$ may satisfy the qualifications described above. The mol fraction of oxygen-particles in figure 24 shows that the atomic form predominates in this temperature range. The second qualification is required in order to determine the source of the anomalous absorption, where the anomalous absorption is the measured absorption minus the classical absorption. The classical absorption of atomic oxygen can be predicted quite accurately since it depends only upon the single collision integral, $\Omega_{\text{o-o}}^{(2.2)}$, calculated by Yun and Mason (ref. 54). The anomalous absorption can then be attributed to either thermal radiation or collisional excitation or both. A calculation shows that the value of $\Delta c_{\text{v}_{\text{exc}}}/R \exp(-\epsilon_1/kT)$ for the first excited level in atomic oxygen can result in an α_{exc} which is larger than α_{class} by a factor of 2, provided a certain range of steric factors can be realized. It may be possible to distinguish the source by comparing the temperature variation of the anomalous ultrasonic absorption with those for α_{rad} and α_{exc} .¹² The distinction is possible since the temperature variations

¹²Relatively accurate values of α_{rad} can be calculated. The main contribution to thermal radiation between $6,000^{\circ}$ and $10,000^{\circ}\text{K}$ comes from atomic line radiation. The corresponding absorption coefficients can be obtained from the data presented by Wilson and Nicolet in reference 32. At the lowest temperatures the mol fraction of molecular oxygen is less than 3×10^{-3} . However, the radiative intensity of the Schumann-Runge band system is so large that its effect must be included. The required spectral absorption coefficients can be found in references 33 and 34. At the highest temperatures the mol fraction of ions and electrons are less than 2×10^{-2} . Again the radiative intensity of a small number of particles becomes important. In this case free-free and free-bound continuum will contribute heavily to the total radiation. The spectral absorption coefficients for the free-bound continuum radiation from O^+ can be obtained from the data presented by Hahne in reference 35, and for the free-free continuum radiation from reference 31. The calculation of α_{exc} for the first excited state of oxygen can be performed in the same manner as described for nitrogen. All but one of the variables in equation (59) can be obtained with a good degree of accuracy. The only variable which cannot be readily calculated or measured is the steric factor, P . Consequently, to obtain a temperature variation of α_{exc} , the assumption must be made that P remains constant between $6,000^{\circ}$ and $10,000^{\circ}\text{K}$. This assumption does not appear to be unreasonable.

of α_{rad} and α_{exc} are entirely different. For example, the radiative coefficient, Q , changes by several orders of magnitude as the temperature increases from $6,000^\circ$ to $10,000^\circ$ K. It is possible for the corresponding α_{rad} to change by several orders of magnitude. In contrast, the product $\Delta c_{\text{vexc}} \tau_{\text{exc}}^{-1}$ and the corresponding α_{exc} probably change by less than one order of magnitude in the same temperature interval.

Early in the report, the statement was made that it may be possible to measure the viscosity or thermal conductivity of nitrogen and argon or both for a large number of conditions, provided other sources of ultrasonic absorption are unimportant. The only basis for this statement was an inspection of the ratio $\alpha_\lambda/\alpha_\eta$. In retrospect, the statement has to be modified because absorption due to relaxation phenomena will mask the classical absorption for a majority of these conditions. The conditions, previously mentioned, are shown in the following table, and the masking phenomena are shown in the last column.

Gas	State	Temperature at $p = 1$ atm, $^\circ\text{K}$	Transport measurement	Masking phenomena
Argon	Atomic	<7,000	Viscosity, thermal conductivity	None
	Partially ionized	8,000-20,000	Viscosity	Ionization relaxation
	Fully ionized	21,000	Thermal conductivity	None
Nitrogen	Molecular	<6,000	Viscosity	Rotational relaxation (ref. 16)
	Dissociated	6,000-10,000	Viscosity	Collisional relaxation ^a
	Partially ionized	10,000-20,000	Viscosity	Collisional relaxation ^a Ionization relaxation
	Fully ionized	21,000	Thermal conductivity	Collisional relaxation ^a

^aDue to excitation of bound electrons.

It can be seen that an accurate measurement of transport coefficients in nitrogen does not seem possible at any temperature. In contrast, transport coefficients of argon can be measured in two regions. In the first region from room temperature to 7000° K, both the viscosity and thermal conductivity of neutral argon can be measured. In the second region where the gas is predominantly electrons and single ions (fig. 2), there is only one other possible source of relaxation absorption. Absorption might be caused by the collective oscillation of free electrons about the less mobile ions. If the

characteristic frequency were lower than the ultrasonic frequency, the oscillations would necessarily be out of phase with the ultrasonic waves, thereby causing some absorption of the ultrasonic energy. However, the characteristic frequency of this electron oscillation is the plasma frequency (ref. 55). For an argon plasma at 20,000° K and 1 atmosphere pressure, the plasma frequency is of the order of 10^{12} cycles per second. This is considerably greater than an ultrasonic frequency of 1 Mc. Consequently, this relaxation absorption due to collective electron oscillations should be negligible. The remaining sources are viscosity and thermal conductivity, with α_λ the predominant mode. The one drawback of this particular measurement is that there is little possibility of determining the temperature variation of α_λ due to the presence of reactive absorption at slightly lower and higher temperatures.

Another gas which may yield information on transport coefficients is hydrogen. The ratio $\alpha_\lambda/\alpha_\eta$ for this gas is shown in figure 25. Meaningful measurements can be obtained in the same two conditions as described for argon - first, where the gas is essentially in the atomic form, and second, where the gas is predominantly electrons and protons. In the first case, for example, the mol fraction of hydrogen atoms at a pressure of one atmosphere is greater than 99 percent from 5,500° to 8,500° K as shown in figure 26. Collisional excitation is not a factor as the first excited level of the hydrogen atom is so far above the ground state [$(\epsilon_1/k) = 118,360^\circ$ K] that the quantity $(\epsilon_1/kT)g_1 \exp(-\epsilon_1/kT)$ in equation (64) is negligible. Consequently, the measured ultrasonic absorption can be attributed to classical sources, viscosity and thermal conductivity. This measurement is essentially a measurement of the collision cross section for the H-H interaction since this is the only cross section which determines both the viscosity and thermal conductivity (eqs. (1) and (2)). This measurement is of fundamental importance since the measured cross section can be compared with the calculated cross section for the H-H interaction. This interaction, in turn, is one of the few atom-atom interactions which can be accurately calculated by quantum-mechanical methods (ref. 56). At higher temperatures where the gas becomes partially ionized, the ratio $\alpha_\lambda/\alpha_\eta$ falls rapidly so that the absorption due to viscosity predominates at relatively high degrees of ionization (~50 percent). Consequently, there is a possibility of measuring the viscosity of a partially ionized gas, provided the absorption due to ionization relaxation is small. This last effect cannot be accurately predicted because the ionization rate constants for hydrogen are unavailable. However, the ionization cross sections in reference 44 indicate that the effect may be small, and can be minimized by increasing the ultrasonic frequency and decreasing the gas pressure. Meaningful measurements can also be made in the region where the majority of the hydrogen atoms are ionized. This occurs at temperatures above 21,000° K for a pressure of 1 atmosphere (fig. 26). In this region there cannot be any internal relaxation phenomenon since the protons are stripped of their electrons. There can be very little ionization relaxation since the mol fraction of hydrogen atoms is less than 1 percent. The only possible source of relaxation absorption is the oscillation of the electrons with respect to the ions, which should be negligible. This leaves the viscosity and thermal conductivity as the only sources of ultrasonic absorption. Since the ratio $\alpha_\lambda/\alpha_\eta$ is much larger than unity, it is possible to measure the thermal conductivity of fully ionized hydrogen over a large temperature range.

CONCLUDING REMARKS

The usefulness of ultrasonic absorption for determining the values of high-temperature gas properties has been evaluated in two steps. First, the ultrasonic absorption coefficients due to various phenomena were calculated over a range of conditions. Second, the magnitudes of the various absorption coefficients were compared to determine if any one of them predominates, as the predominance of the one absorption coefficient is required for an accurate determination of the corresponding gas property. The sources of ultrasonic absorption considered are viscosity and thermal conductivity (classical absorption), thermal radiation, and relaxation effects due to molecular vibration, atomic collisional excitation of bound electrons, dissociation, and ionization. The range of conditions used in these calculations includes those found in Carnevale's experiments with argon and with nitrogen. This range was chosen to provide an experimental check of the calculations and to provide a further interpretation of experimental results. Ultrasonic absorption in other atmospheric constituents such as oxygen and hydrogen was also considered. The following are the results of the calculations.

The existing relationship between transport coefficients and the classical absorption coefficient, α_{class} , is valid for a reactive gas provided the proper thermodynamic and transport properties are used. This relationship shows that it is not possible to measure the predominant component of the thermal conductivity - the reactive component - due to a compensating increase in the reactive component of the specific heat. However, it is possible to obtain transport coefficients of certain gases for two states from ultrasonic absorption measurements. These measurements can only be accomplished for two gases, argon and hydrogen. The first state occurs when the gas particles are predominantly in the atomic form. The measurement of a single quantity - the classical absorption - will yield accurate values of both the viscosity and thermal conductivity. The measurements in the two gases can be made over a wide range of temperatures. The second state occurs when the gas particles are comprised mainly of electrons and single ions. In this case the simultaneous determination of the viscosity and thermal conductivity is not feasible because of the increase in the number of different types of particle interactions. However, the thermal conductivity of an argon plasma can be measured over a narrow range of temperatures and the thermal conductivity of a hydrogen plasma can be measured over a wide range of temperatures. The measurements should provide sufficient information for verification of the expressions for the transport coefficients of an ionized gas. The transport coefficients of nitrogen and oxygen cannot be measured with any degree of accuracy at any temperature because α_{class} is masked by relaxation effects.

Carnevale showed that his measured ultrasonic absorption coefficients are larger than α_{class} by almost an order of magnitude at the higher temperatures. These anomalous values of the absorption coefficient appear at temperatures as low as 6,000° K for nitrogen and 10,000° K for argon. Carnevale suggests that anomalous absorption is caused by the transfer of spectral radiative energy within an ultrasonic wavelength. Order-of-magnitude arguments described in this report have shown that these anomalous absorptions cannot be attributed

to thermal radiation. These arguments were verified by calculating the radiative induced absorption, α_{rad} , in nitrogen using approximate radiative emission coefficients. For a pressure of 1 atmosphere the value of α_{rad} was smaller than α_{class} by 5 orders of magnitude at 6,000° K, by 3 orders of magnitude at 10,000° K, and by 1 order of magnitude at 20,000° K. From these calculations and a cursory examination of the radiative properties of other gases, it is concluded that the ultrasonic absorption technique is not capable of measuring spectral intensities of atmospheric gases below temperatures of 25,000° K.

The only remaining phenomena which can account for the difference between the measured and classical values of the ultrasonic absorption are the relaxation phenomena. An examination of the energies and relaxation times associated with the phenomena showed that the only possible source of the anomalous ultrasonic absorption in argon is ionization relaxation. Calculations showed that α_{ion} is 10 times larger than α_{class} at the temperature where ionization effects are at a maximum. The calculated values of the total absorption, $\alpha_{\text{class}} + \alpha_{\text{ion}}$, compare favorably with the measured absorption. From this, it is concluded that ionization relaxation may be the cause of anomalous absorption in argon, although a positive identification is not possible because of the large scatter in the experimental data. It is also concluded that the ultrasonic absorption technique may be a useful means of accurately measuring the predominant ionization rate constant of argon.

The same type of calculation for nitrogen showed that the value of α_{ion} is twice as large as the value of α_{class} at the temperature where ionization effects are at a maximum. However, ionization relaxation cannot account for the large anomalous absorption at lower temperatures (6,000°-12,000° K at a pressure of 1 atmosphere) where ionization effects disappear. An examination of the energies and relaxation times associated with other relaxation phenomena showed that the anomalous absorption in this region is possibly caused by collisional excitation of nitrogen atoms and ions. Calculations showed that the corresponding excitation time is consistent with the collision frequency. However, it would require a fairly high collisional efficiency - roughly 1 transition out of every 7 sufficiently energetic collisions. Whether this number is reasonable cannot be checked at the present time, because the excitation cross sections have not been calculated or measured. It may be possible to corroborate the dominance of collisional excitation by measuring absorption in atomic oxygen. The advantage of the measurement in oxygen is the much wider temperature range where the particles are in the atomic form.

It is obvious from the above remarks that with one exception, no generalizations can be made on the usefulness of the ultrasonic absorption technique for measuring transport properties and relaxation phenomena. The only exception is that it cannot be used to measure spectral intensities of atmospheric gases. The fact that the technique accurately measures certain high temperature properties for one gas does not necessarily mean that it will measure

the same properties for another gas. An order of magnitude calculation must be made prior to the measurements to determine which properties can be measured for a given gas.

Ames Research Center

National Aeronautics and Space Administration

Moffett Field, Calif., 94035, Nov. 22, 1967

129-01-02-01-00-21

REFERENCES

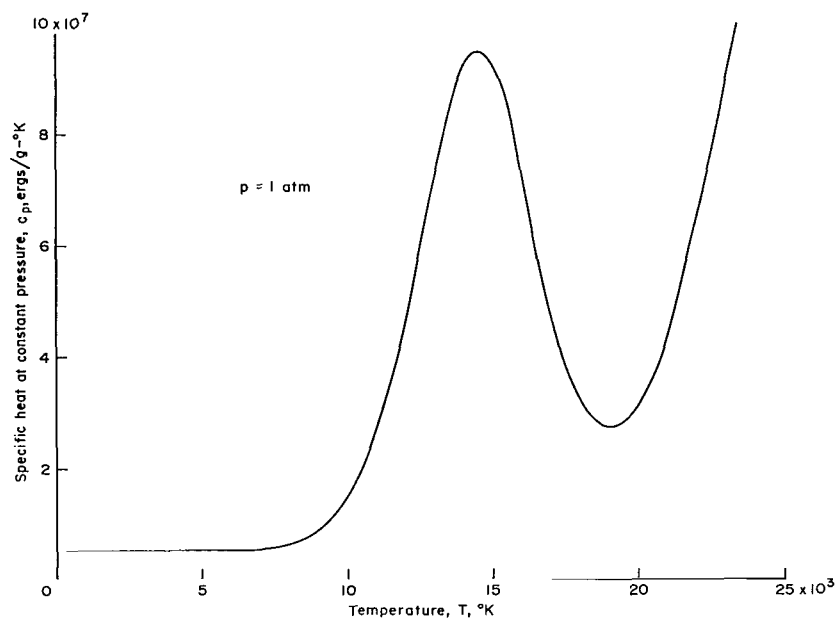
1. Maecker, H.: The Properties of Nitrogen to 15,000° K. AGARD Rep. 324, 1959.
2. Lin, Shao-Chi; Resler, E. L.; and Kantrowitz, Arthur: Electrical Conductivity of Highly Ionized Argon Produced by Shock Waves. J. Appl. Phys., vol. 26, no. 1, Jan. 1955, pp. 95-109.
3. Millikan, Roger C.; and White, Donald R.: Systematics of Vibrational Relaxation. J. Chem. Phys., vol. 39, no. 12, Dec. 15, 1963, pp. 3209-3213.
4. Hansen, C. Frederick: Estimates for Collision-Induced Dissociation Rates. AIAA J., vol. 3, no. 1, Jan. 1965, pp. 61-66.
5. Petschek, Harry; and Byron, Stanley: Approach to Equilibrium Ionization Behind Strong Shock Waves in Argon. Ann. Phys., vol. 1, no. 3, June 1957, pp. 270-315.
6. Wong, H.; and Bershader, D.: Thermal Equilibration Behind an Ionizing Shock. J. Fluid Mech., vol. 26, pt. 3, 1966, pp. 459-479 plus plate I.
7. Wilson, J.: Ionization Rate of Air Behind High-Speed Shock Waves. Phys. Fluids, vol. 9, no. 10, Oct. 1966, pp. 1913-1921.
8. AVCO Corporation: Theoretical and Experimental Studies of High-Temperature Gas Properties. Tech. Rep. RAD-TR-65-7, May 1965.
9. Markham, Jordan J.; Beyer, Robert T.; and Lindsay, R. B.: Absorption of Sound in Fluids. Rev. Mod. Phys., vol. 23, no. 4, Oct. 1951, pp. 353-411.
10. Richardson, E. G.: Absorption and Velocity of Sound in Vapors. Rev. Mod. Phys., vol. 27, no. 1, Jan. 1955, pp. 15-25.
11. Herzfeld, Karl F.; and Litovitz, Theodore A.: Absorption and Dispersion of Ultrasonic Waves. Academic Press, N. Y., 1959.
12. Einstein, Albert: Schallausbreitung in Teilweise Dissoziierten Gasen. Akademie der wissenschaften, Berlin, Sitzungsherichte, 1920, pp. 380-385.
13. Kneser, H. O.; and Gauler, O.: Das Problem der Schallausbreitung in Teilweise Dissoziierten Gasen. Physik. Z., vol. 37, no. 19, Oct. 1936, pp. 677-684.
14. Stokes, G. G.: An Examination of the Possible Effect of the Radiation of Heat on the Propagation of Sound. Phil. Mag., vol. 1 - Fourth Series, 1851, pp. 305-317.

15. Rayleigh, John William S.: Theory of Sound. London, Macmillan, 1937.
16. Carnevale, E. H.; Larson, G.; Lynnworth, L. C.; Carey, C.; Panaro, M.; and Marshall, T.: Experimental Determination of Transport Properties of High Temperature Gases. NASA CR-789, 1967.
17. Hunt, Frederick V.: Notes on the Exact Equations Governing the Propagation of Sound in Fluids. J. Acoust. Soc. Am., vol. 27, no. 6, Nov. 1955, pp. 1019-1039.
18. Hilsenrath, Joseph; Beckett, Charles W.; Benedict, William S.; Fano, Lilla; Hoge, Harold J.; Masi, Joseph F.; Nuttall, Ralph L.; Touloukian, Yeram S.; and Woolley, Harold W.: Tables of Thermodynamic and Transport Properties of Air, Argon, Carbon Dioxide, Carbon Monoxide, Hydrogen, Nitrogen, Oxygen, and Steam. Pergamon Press, N. Y., 1960.
19. Drellishak, K. S.; Knopp, C. F.; and Cambel, Ali Bulent: Partition Functions and Thermodynamic Properties of Argon Plasma. AEDC-TDR-63-146, 1963.
20. Drellishak, K. S.; Aeschliman, D. P.; and Cambel, Ali Bulent: Tables of Thermodynamic Properties of Argon, Nitrogen, and Oxygen Plasmas. AEDC-TDR-64-12, 1964.
21. Hirschfelder, Joseph O.; Curtiss, Charles F.; and Bird, R. Byron: Molecular Theory of Gases and Liquids. John Wiley and Sons, Inc., N. Y., 1954.
22. Chapman, Sydney; and Cowling, T. G.: The Mathematical Theory of Non-Uniform Gases. Second ed., Cambridge Univ. Press, London, 1952.
23. Mason, E. A.; and Monchick, L.: Heat Conductivity of Polyatomic and Polar Gases. J. Chem. Phys., vol. 36, no. 6, March 15, 1962, pp. 1622-1639.
24. Butler, James N.; and Brokaw, Richard S.: Thermal Conductivity of Gas Mixtures in Chemical Equilibrium. J. Chem. Phys., vol. 26, no. 6, June 1957, pp. 1636-1643.
25. Ahtye, Warren F.: A Critical Evaluation of Methods for Calculating Transport Coefficients of Partially and Fully Ionized Gases. NASA TN D-2611, 1965.
26. Ahtye, Warren F.: Total Thermal Conductivity of Partially and Fully Ionized Gases. Phys. Fluids, vol. 8, no. 10, Oct. 1965, pp. 1918-1920. (Erratum, vol. 9, no. 1, Jan. 1966, p. 224.)
27. Hansen, C. Frederick: Approximations for the Thermodynamic and Transport Properties of High-Temperature Air. NASA TR R-50, 1959.

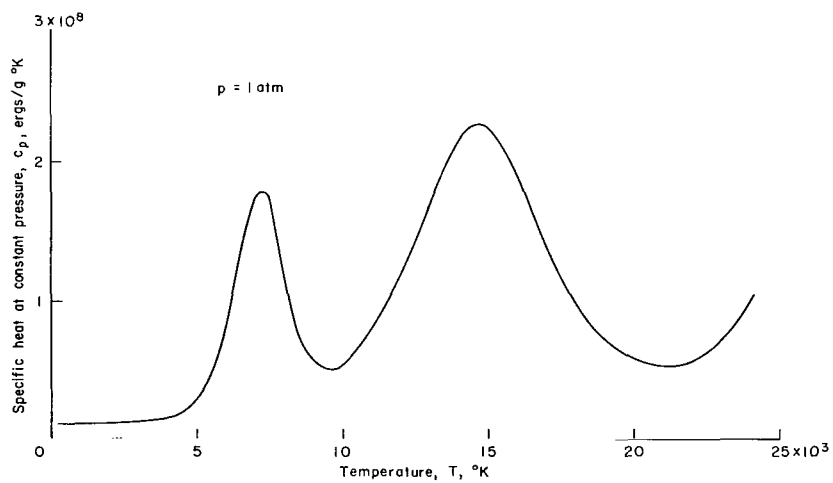
28. Yun, Kwang-Sik; Weissman, Stanley; and Mason, E. A.: High-Temperature Transport Properties of Dissociating Nitrogen and Dissociating Oxygen. *Phys. Fluids*, vol. 5, no. 6, June 1962, pp. 672-678.
29. Yos, Jerrold M.: Transport Properties of Nitrogen, Hydrogen, Oxygen, and Air to 30,000° K. AVCO Rep. RAD TM-63-7, 1963.
30. Smith, P. W., Jr.: Effect of Heat Radiation on Sound Propagation in Gases. *J. Acoust. Soc. Am.*, vol. 29, no. 6, June 1957, pp. 693-698.
31. Sewell, K. G.: The Radiative Properties of Air in Thermodynamic Equilibrium. Ling-Temco-Vought Research Center Rep. No. 0-71000/2R-26, 1962.
32. Wilson, K. H.; and Nicolet, W. E.: Spectral Absorption Coefficients of Carbon, Nitrogen, and Oxygen Atoms. Lockheed Missiles and Space Co. LMSC-4-17-66-5, 1966.
33. Breene, R. G., Jr.; and Nardone, Maria: Radiant Emission from High Temperature Equilibrium Air. General Electric, Missile and Space Div. Rep. No. GE R61S020, 1961.
34. Churchill, D. R.; Armstrong, B. H.; and Mueller, K. G.: Absorption Coefficients of Heated Air: A Compilation to 24,000° K. Vols. I and II, Lockheed Missiles and Space Co. LMSC-4-77-65-1 and LMSC-4-77-65-2, 1965.
35. Hahne, Gerhard E.: The Vacuum Ultraviolet Radiation From N^{+-} and O^{+-} -Electron Recombination in High-Temperature Air. NASA TN D-2794, 1965.
36. Biberman, L. M.; Akubov, I. T. I.; Norman, G. E.; and Vorobyov, V. S.: Radiation Heating Under Hypersonic Flow. *Astronautica Acta*, vol. X, Fasc. 3-4, 1964, pp. 238-252.
37. Shields, F. Douglas: Sound Absorption in the Halogen Gases. *J. Acoust. Soc. Am.*, vol. 32, no. 2, Feb. 1960, pp. 180-185.
38. Damköhler, Gerhard: Isentropic Phase Changes in Dissociating Gases and the Method of Sound Dispersion for the Investigation of Homogeneous Gas Reactions With Very High Speed. NACA TM 1268, 1950.
39. Pritchard, H. O.: The Dissociation of Diatomic Molecules and the Recombination of Atoms. *J. Phys. Chem.*, vol. 66, no. 11, Nov. 1962, pp. 2111-2113.
40. Byron, Stanley: Shock-Tube Measurement of the Rate of Dissociation of Nitrogen. *J. Chem. Phys.*, vol. 44, no. 4, Feb. 15, 1966, pp. 1378-1388.

41. Allen, R. A.; Keck, J. C.; and Camm, J. C.: Nonequilibrium Radiation and the Recombination Rate of Shock-Heated Nitrogen. *Phys. Fluids*, vol. 5, no. 3, March 1962, pp. 284-291.
42. Maier-Leibnitz, H.: Ausbeutemessungen Beim Stob Langsamer Electronen mit Edelgasatomen. *Z. Physik*, vol. 95, 7-8, June 26, 1935, pp. 499-523.
43. Kollath, R.: Influence of Angular Distribution of Scattered Electrons on the Measurement of the Effective Cross Section. (Der Einfluss der Winkelverteilung Gestreuter Electronen auf die Messung des Wirkungsquerschnittes.) *Ann. Physik*, vol. 15, no. 5, Dec. 1932, pp. 485-515.
44. McDaniel, Earl W.: *Collision Phenomena in Ionized Gases*. John Wiley and Sons, Inc., N. Y., 1964.
45. Hasted, J. B.: *Physics of Atomic Collisions*. Butterworths Inc., Washington, D. C., 1964.
46. Harwell, Kenneth E.; and Jahn, Robert G.: Initial Ionization Rates in Shock-Heated Argon, Krypton, and Xenon. *Phys. Fluids*, vol. 7, no. 2, Feb. 1964, pp. 214-222.
47. Appleton, J. P.: Electrical Precursors of Ionizing Shock Waves. *Phys. Fluids*, vol. 9, no. 2, Feb. 1966, pp. 336-342.
48. Bortner, M. H.: Chemical Kinetics in a Reentry Flow Field. General Electric Space Sciencies Laboratory Report No. R63SD63, 1963.
49. Moore, Charlotte E.: Atomic Energy Levels. Vol. 1, Nat. Bur. Stds., Circular 467, June 15, 1949.
50. Vigoreaux, P.: *Ultrasonics*. John Wiley and Sons, Inc., N. Y., 1951.
51. Glasstone, Samuel: *Theoretical Chemistry*. D. Van Nostrand Co., Inc., N. Y., 1944.
52. Vincenti, Walter G.; and Kruger, Charles H., Jr.: *Introduction to Physical Gas Dynamics*. John Wiley and Sons, Inc., N. Y., 1965.
53. Von Engel, Alfred Hans: *Ionized Gases*, Oxford University Press, London, 1955.
54. Yun, K. S.; and Mason, E. A.: Collision Integrals for the Transport Properties of Dissociating Air at High Temperatures. *Phys. Fluids*, vol. 5, no. 4, April 1962, pp. 380-386.
55. Spitzer, Lyman, Jr.; and Härm, Richard: Transport Phenomena in a Completely Ionized Gas. *Phys. Rev.*, vol. 89, no. 5, March 1953, pp. 977-981.

56. Dalgarno, A.; and Lynn, N.: Resonance Forces at Large Separations.
Proc. Phys. Soc. A, vol. 69, Part 11, no. 443A, Nov. 1956, pp. 821-829.

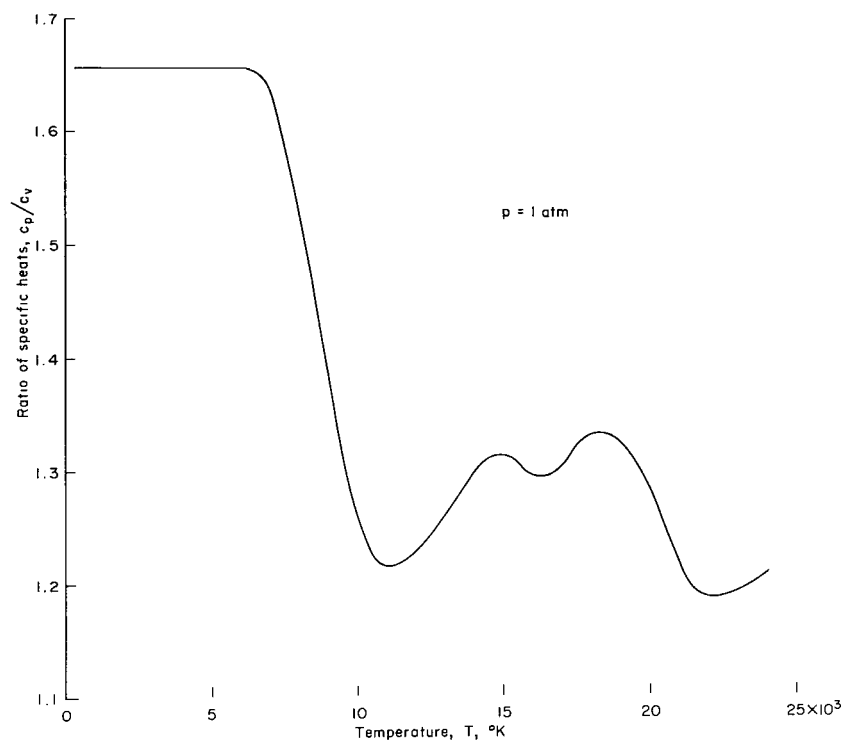


(a) Argon.

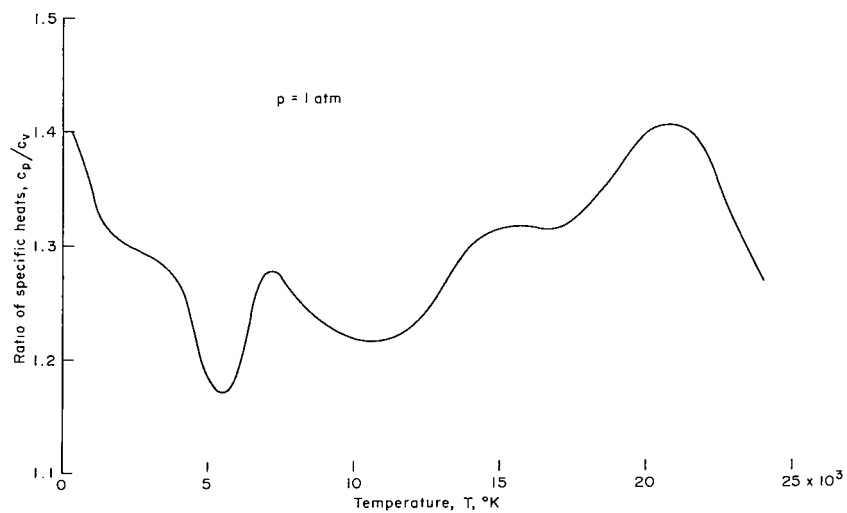


(b) Nitrogen.

Figure 1.- Specific heat at constant pressure as a function of temperature.

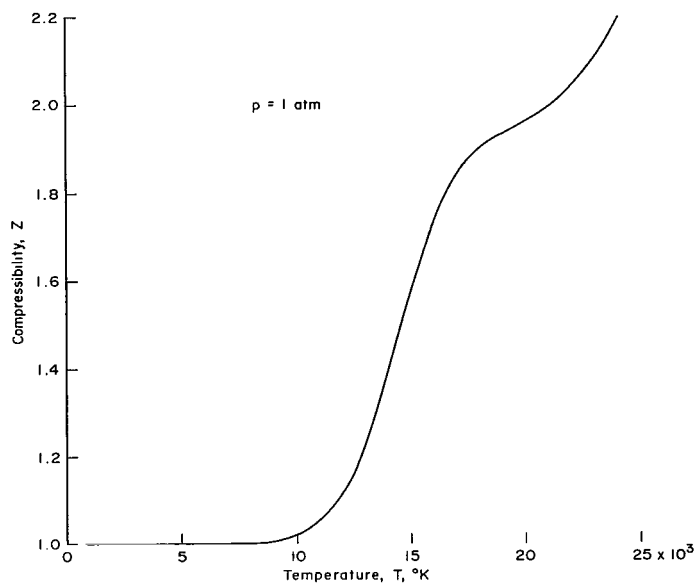


(a) Argon.

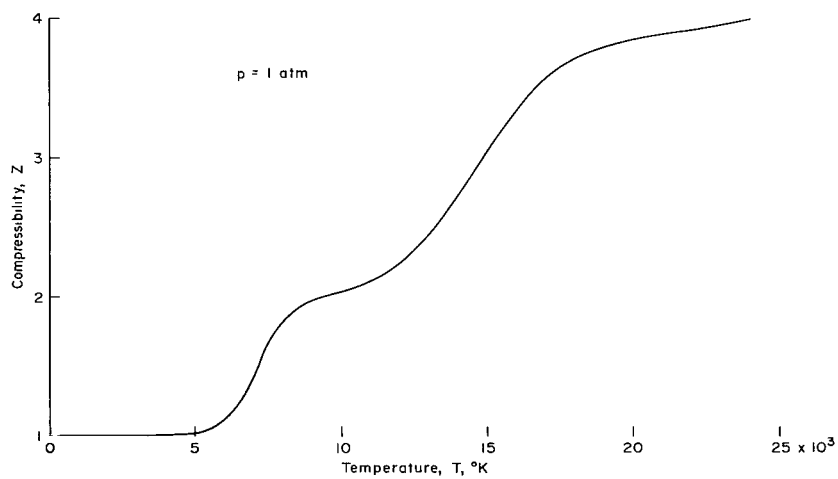


(b) Nitrogen.

Figure 2.- Ratio of specific heats as a function of temperature.

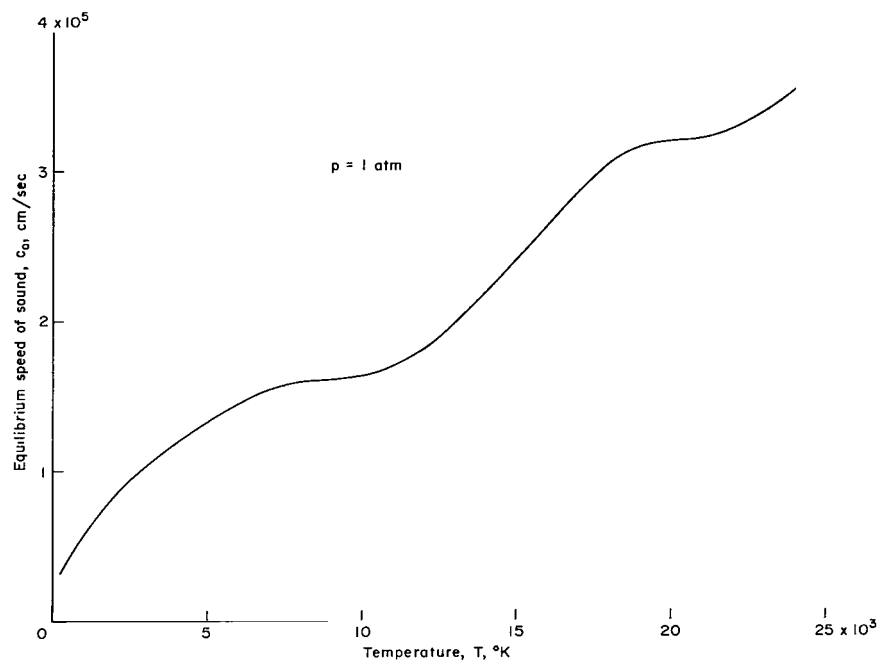


(a) Argon.

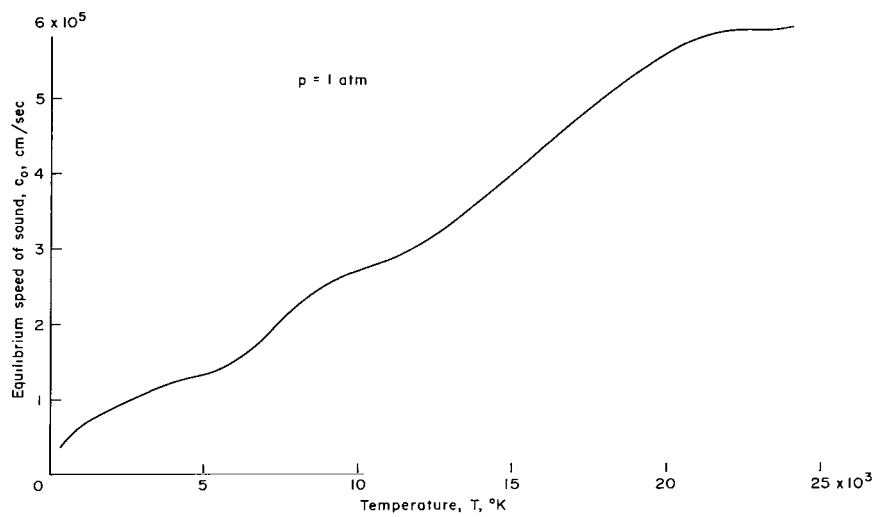


(b) Nitrogen.

Figure 3.- Compressibility as a function of temperature.

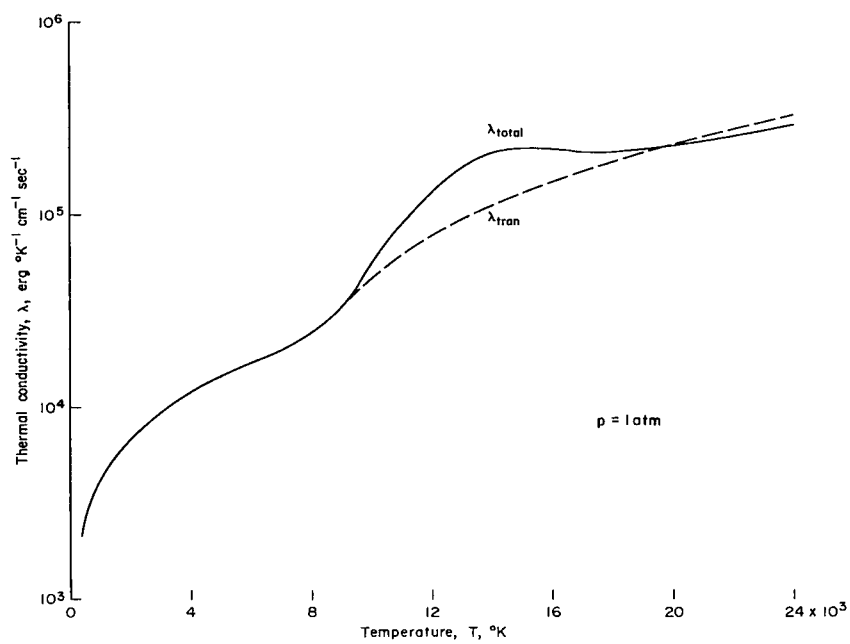


(a) Argon.

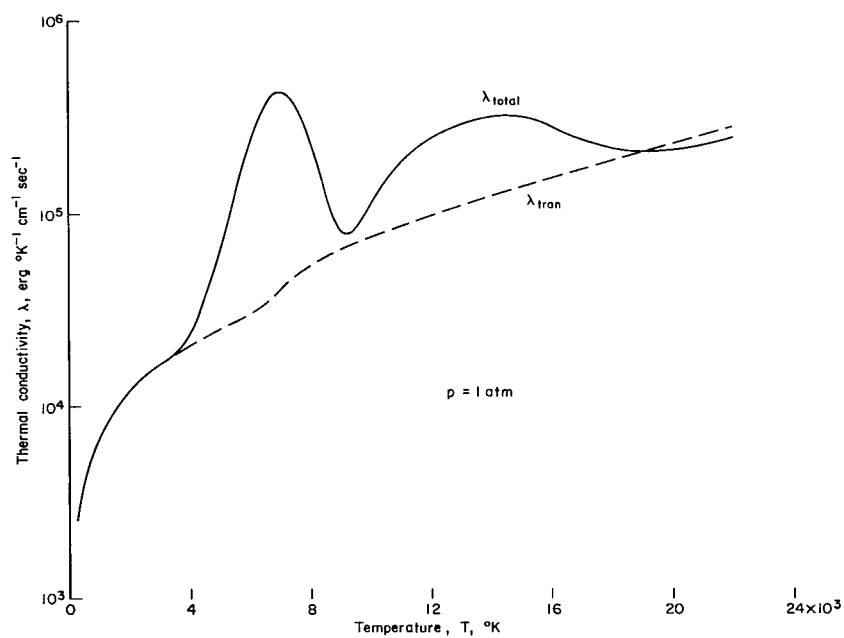


(b) Nitrogen.

Figure 4.- Equilibrium speed of sound as a function of temperature.

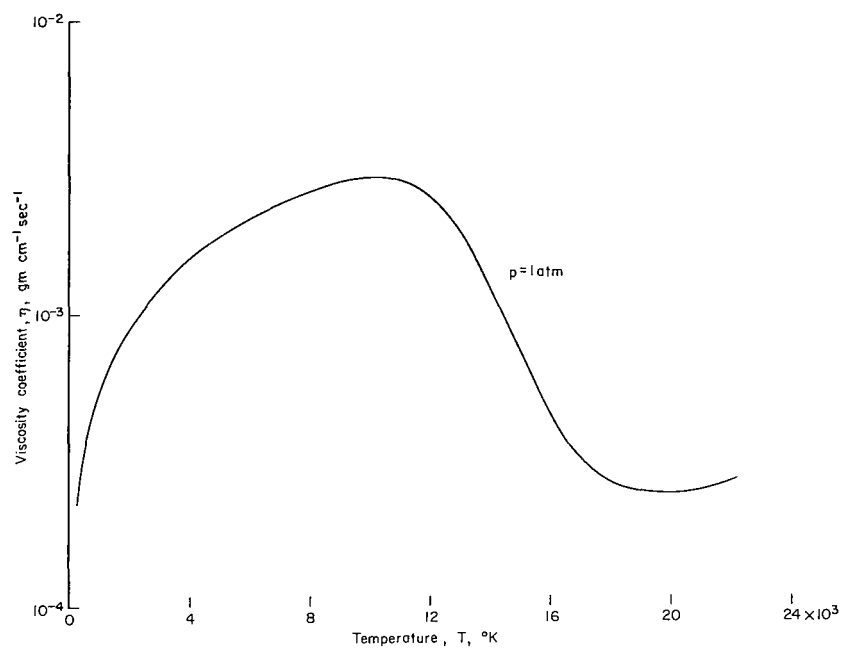


(a) Argon.

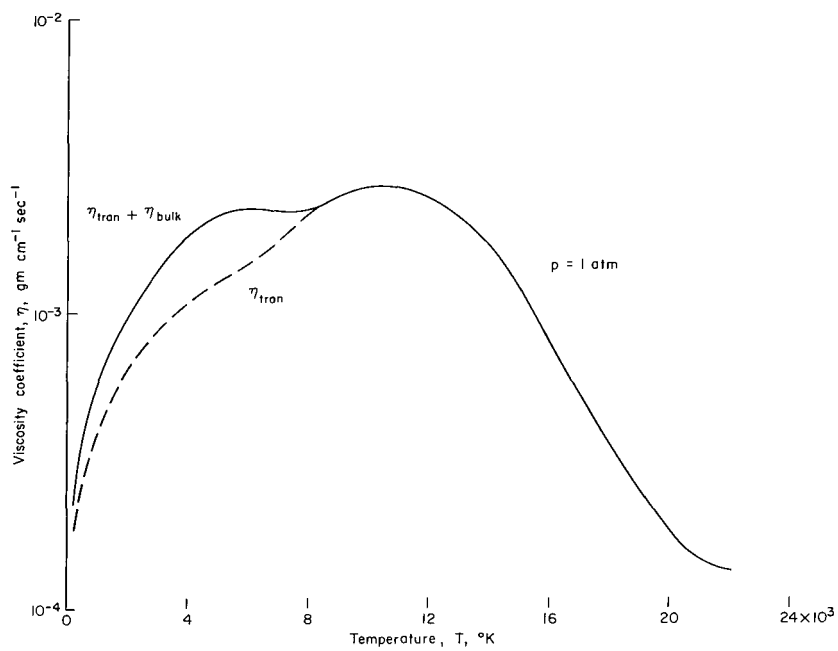


(b) Nitrogen.

Figure 5.- Thermal conductivity as a function of temperature.

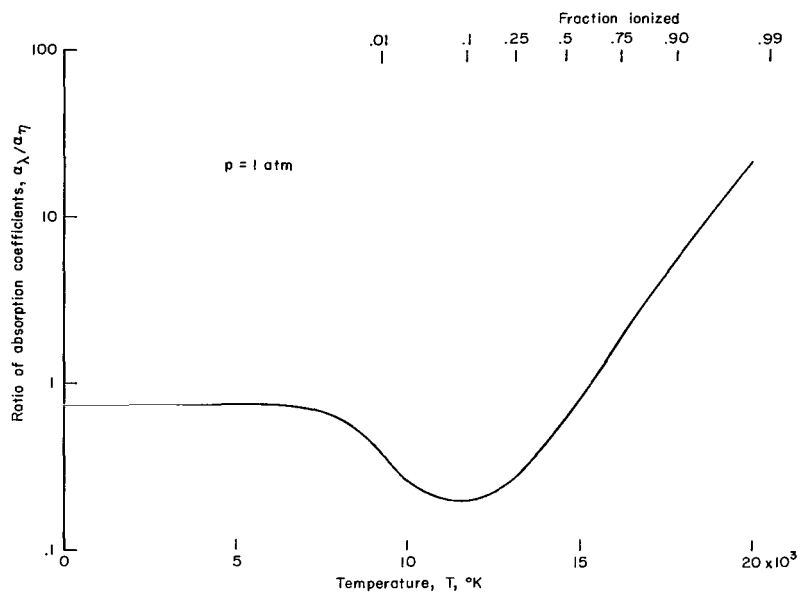


(a) Argon.

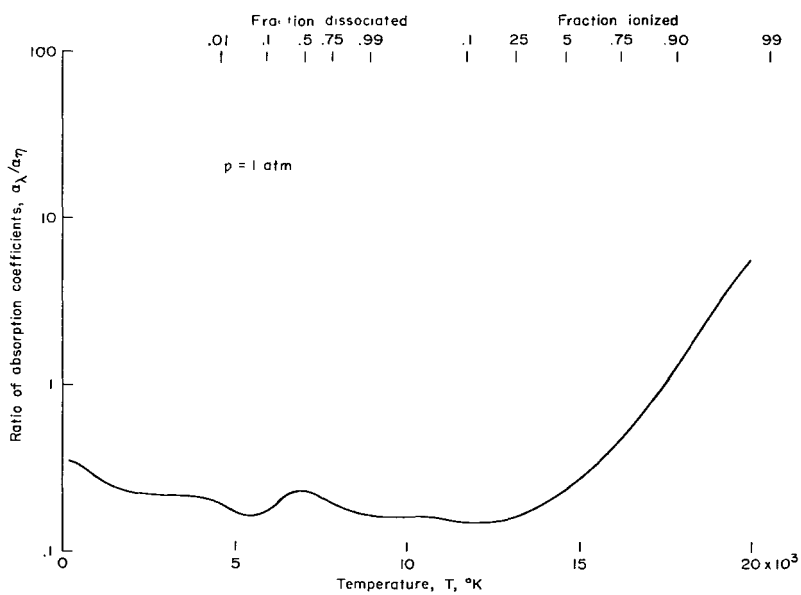


(b) Nitrogen.

Figure 6.- Viscosity coefficient as a function of temperature.

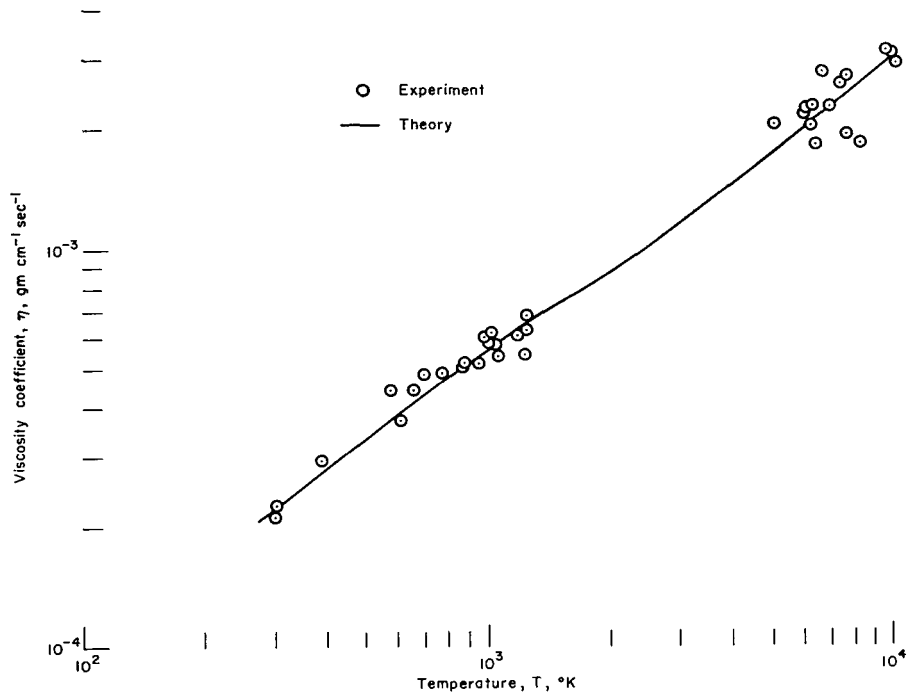


(a) Argon.

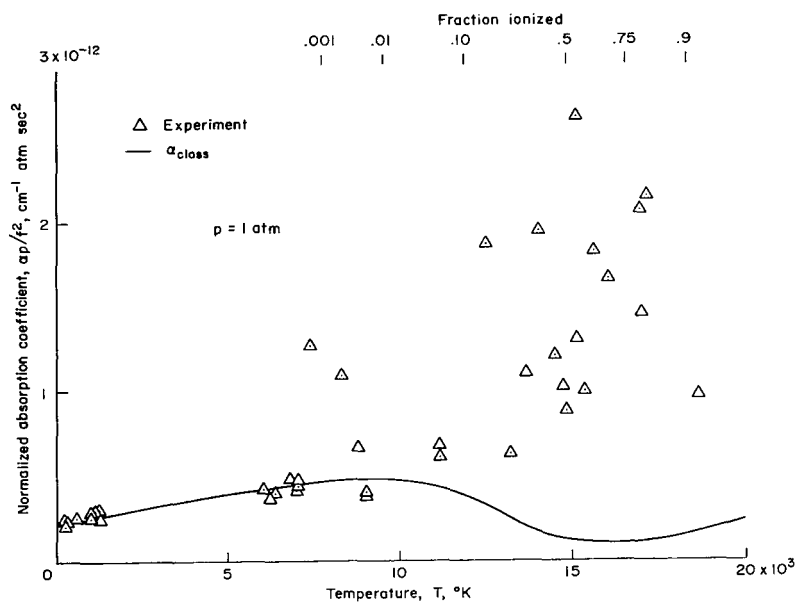


(b) Nitrogen.

Figure 7.- Comparison of ultrasonic absorption due to thermal conductivity and viscosity.

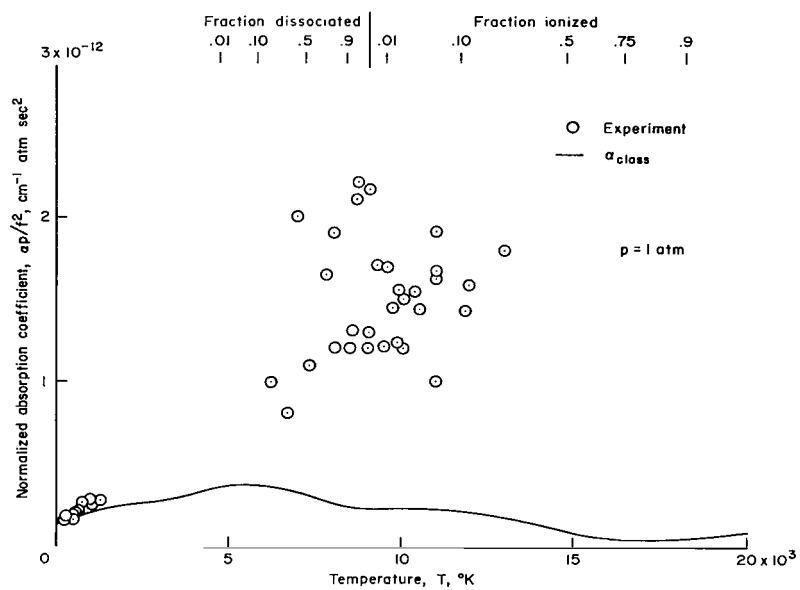


(a) Viscosity vs. temperature.



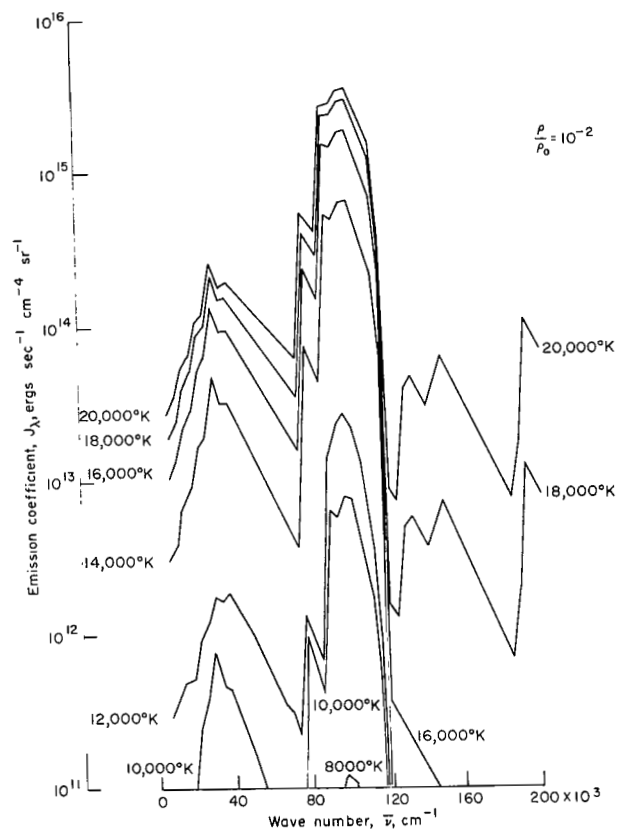
(b) Argon.

Figure 8.- Comparison of measured and classical values of ultrasonic absorption.

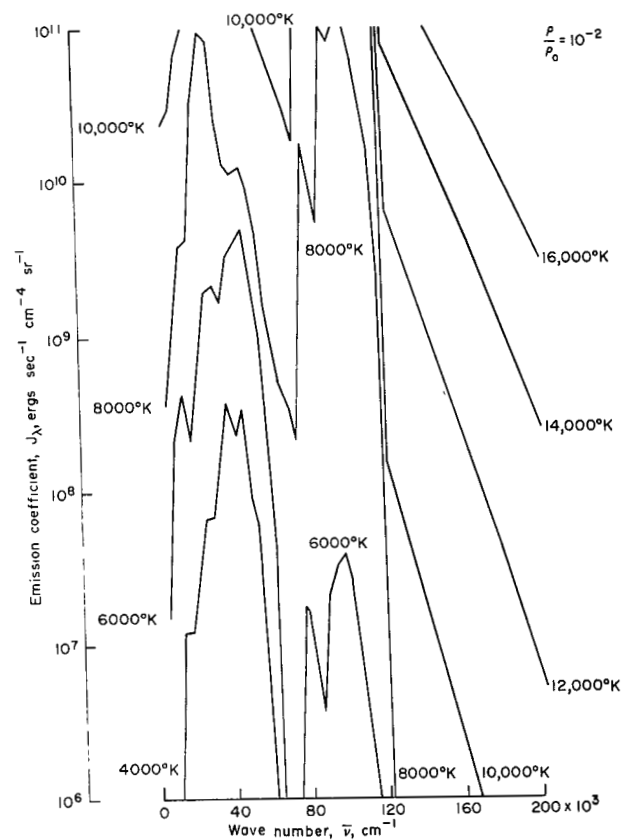


(c) Nitrogen.

Figure 8.- Concluded.



(a) $T = 8,000^{\circ} \text{ K to } 20,000^{\circ} \text{ K.}$



(b) $T = 4,000^{\circ} \text{ K to } 16,000^{\circ} \text{ K.}$

Figure 9.- Spectral emission coefficient of air.

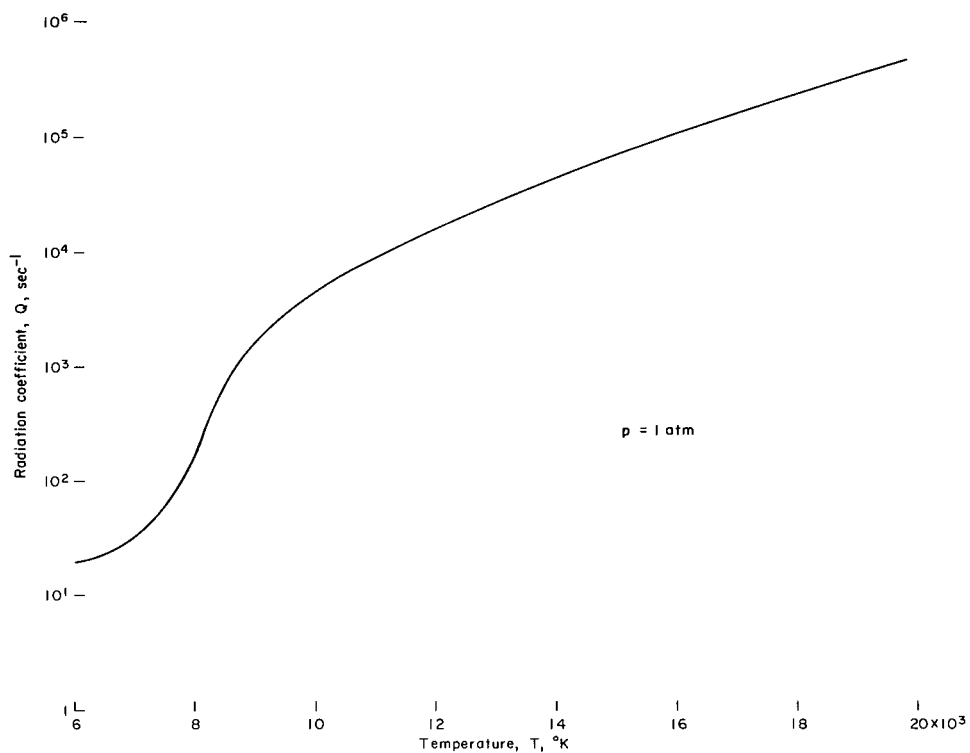


Figure 10.- Radiation coefficient as a function of temperature.

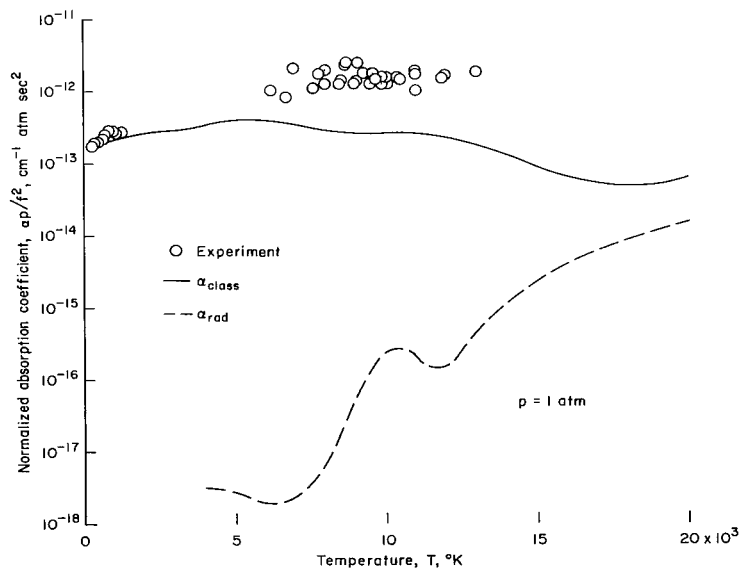


Figure 11.- Effect of thermal radiation on ultrasonic absorption in nitrogen.

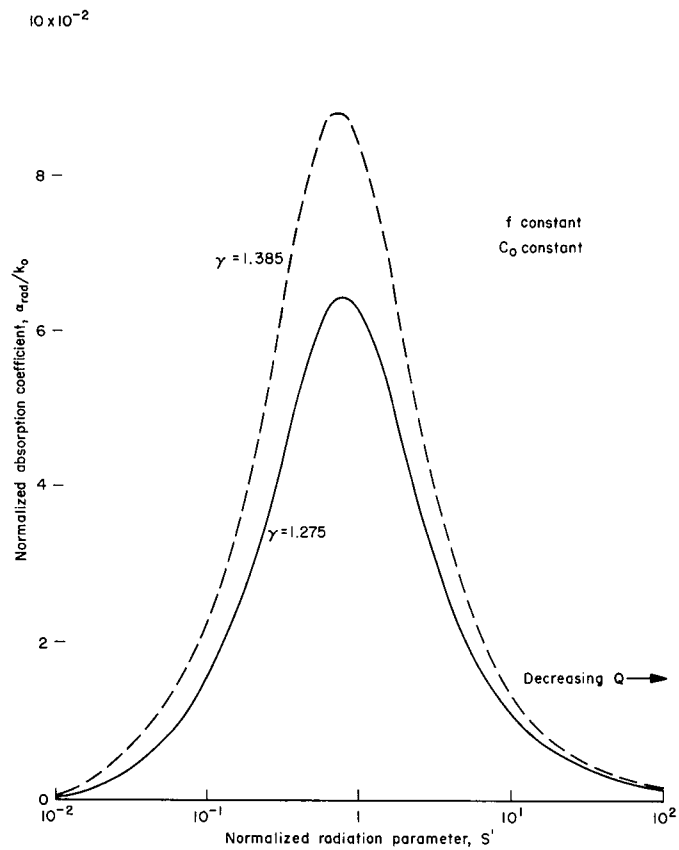


Figure 12.- Effect of varying thermal radiation.

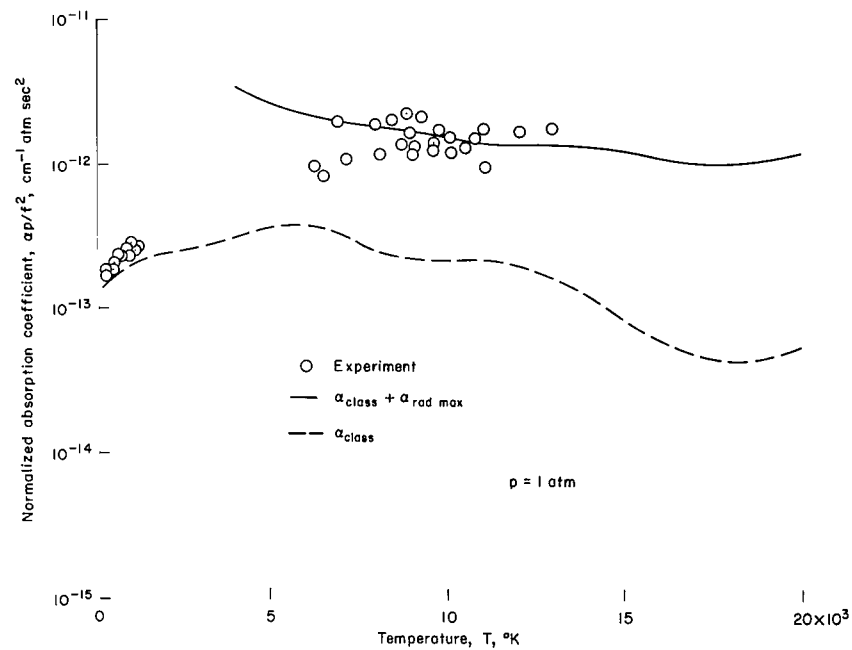


Figure 13.- Effect of radiative maximum.

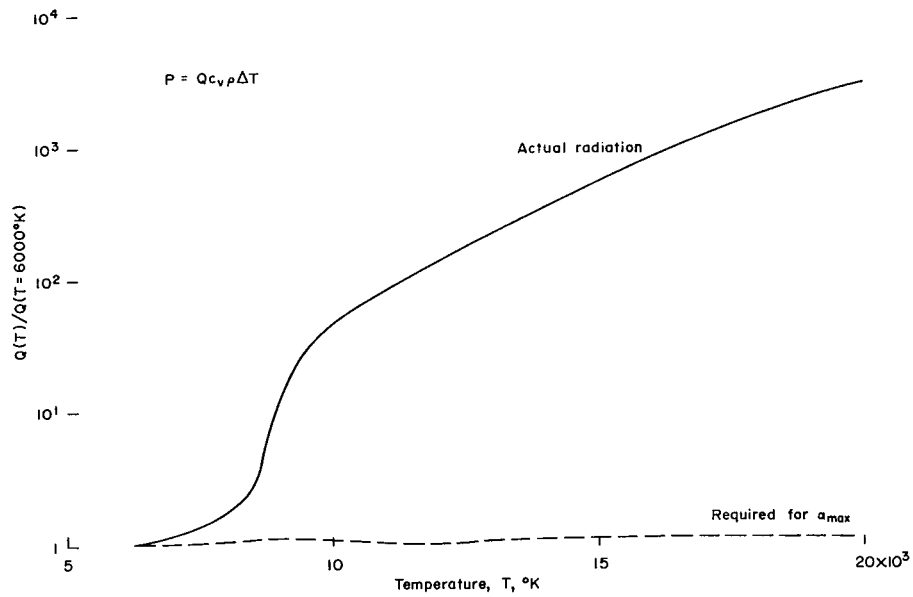


Figure 14.- Temperature variation of radiative power.

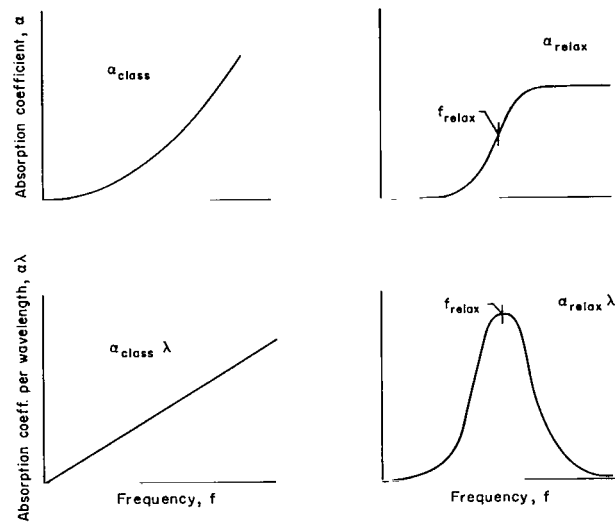


Figure 15.- Effect of frequency on absorption parameters.

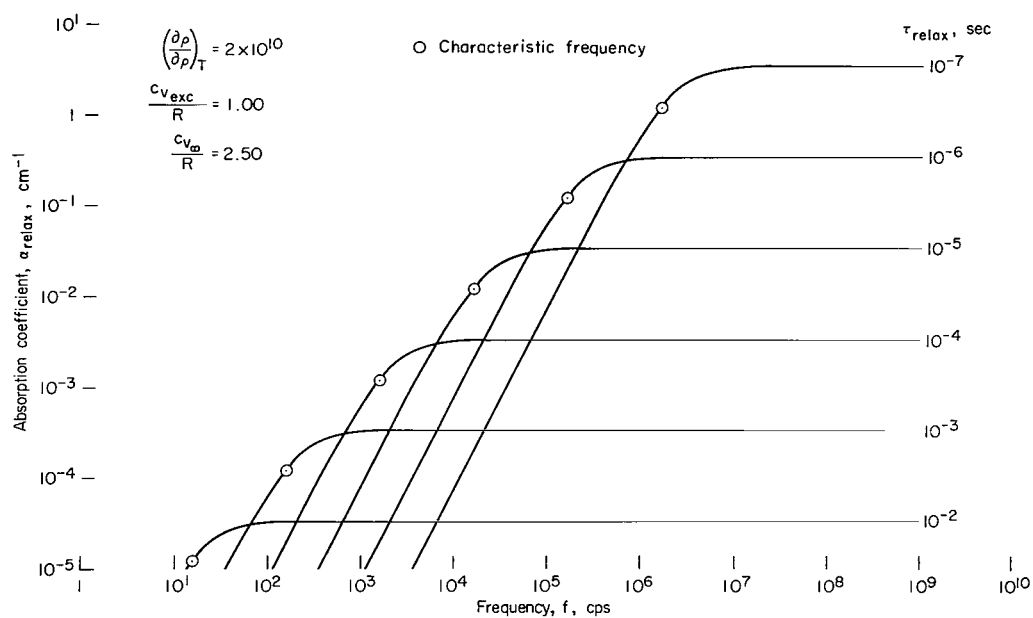


Figure 16.- Variation of relaxation absorption with ultrasonic frequency and relaxation time.

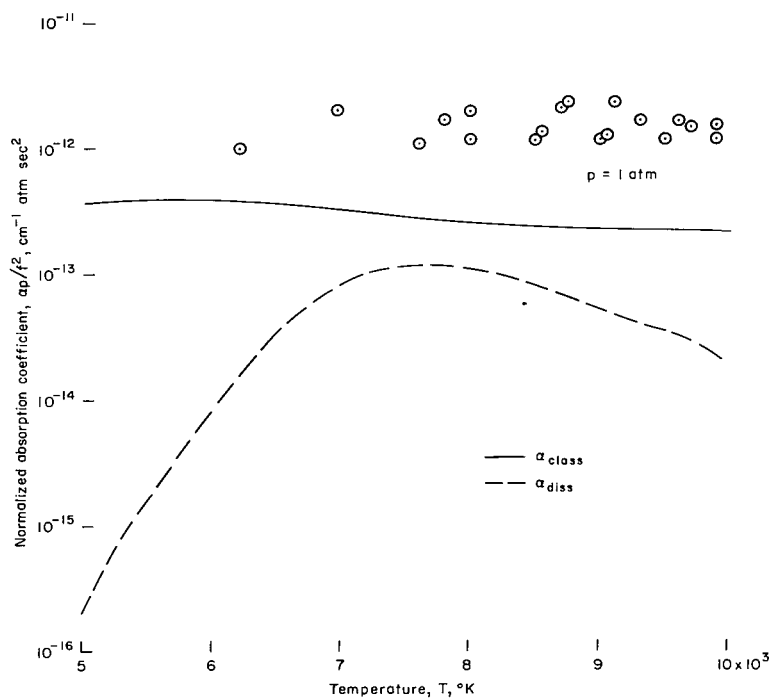


Figure 17.- Comparison of classical and dissociative absorption in nitrogen.

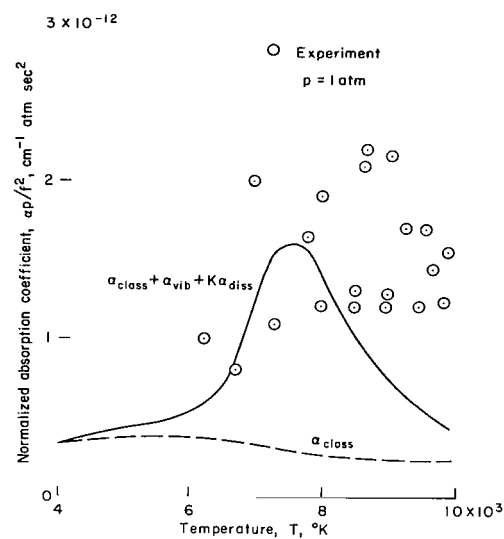


Figure 18.- Effect of arbitrary increase in dissociation rate constant.

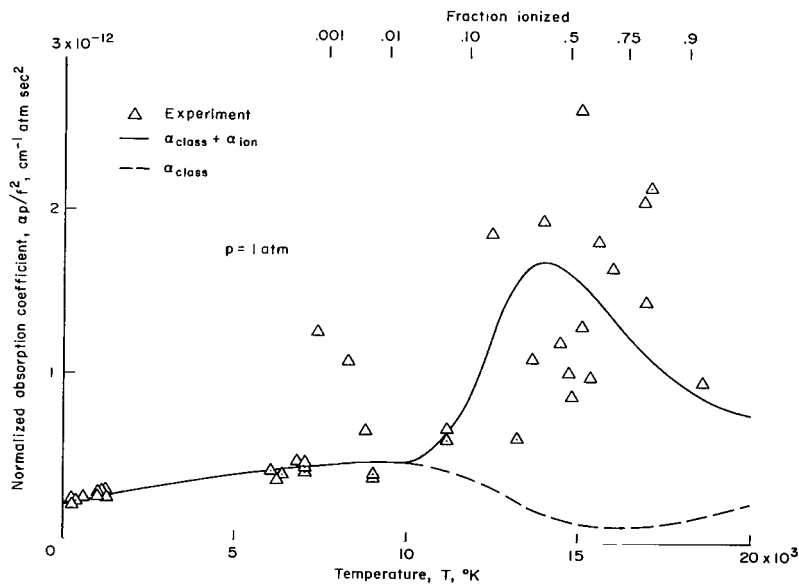


Figure 19.- Effect of ionization relaxation.

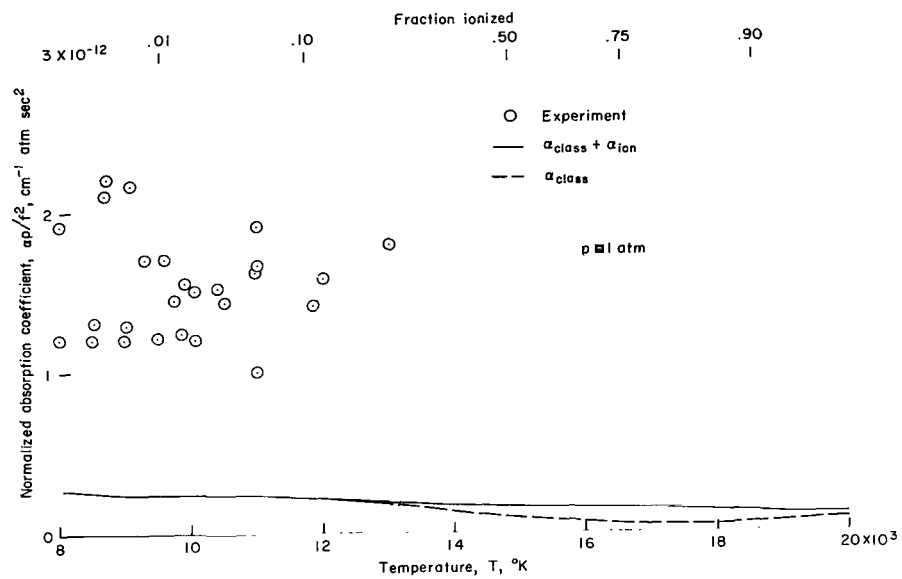
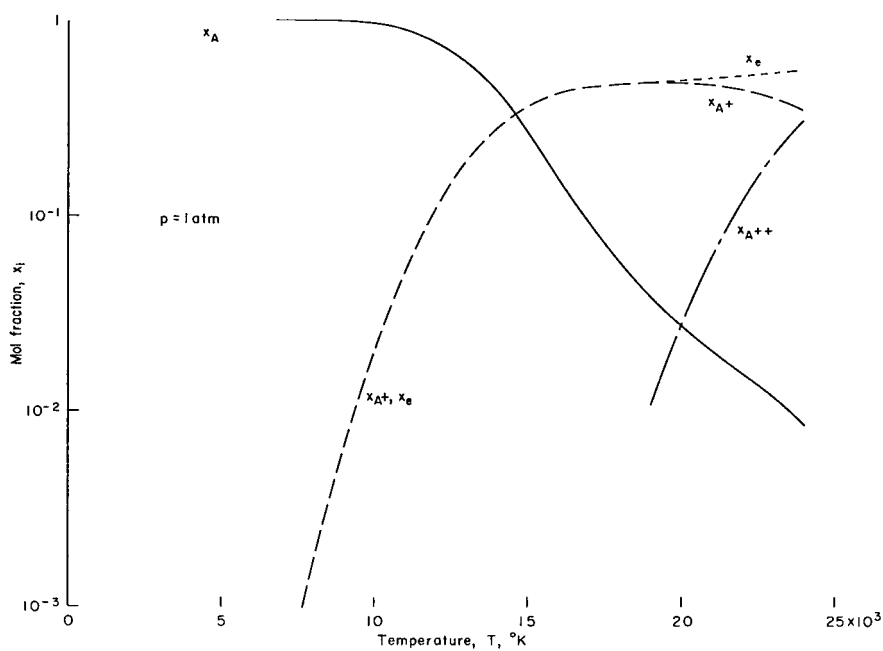
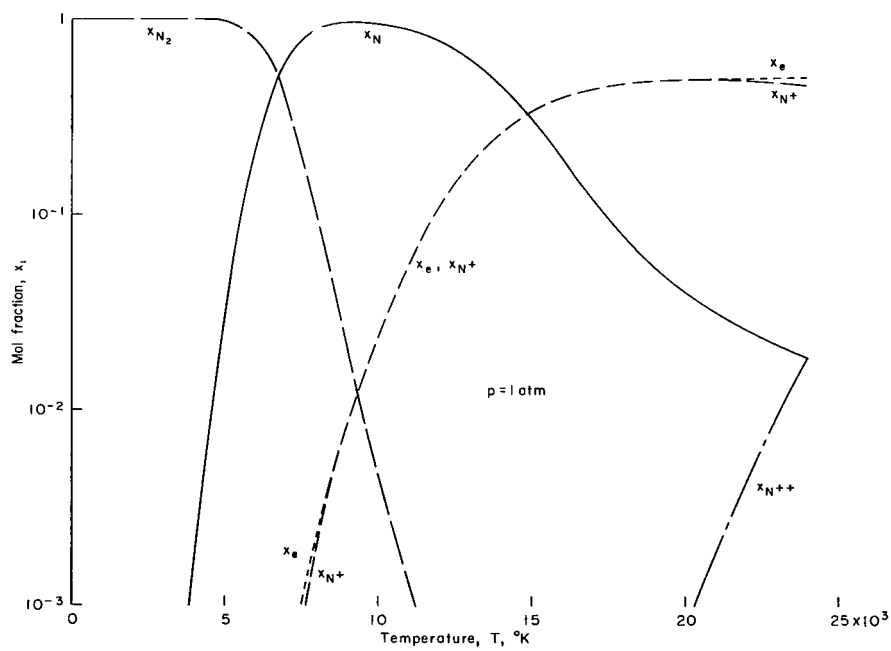


Figure 20.- Effect of ionization relaxation in nitrogen.



(a) Nitrogen.



(b) Argon.

Figure 21.- Mol fractions as a function of temperature.

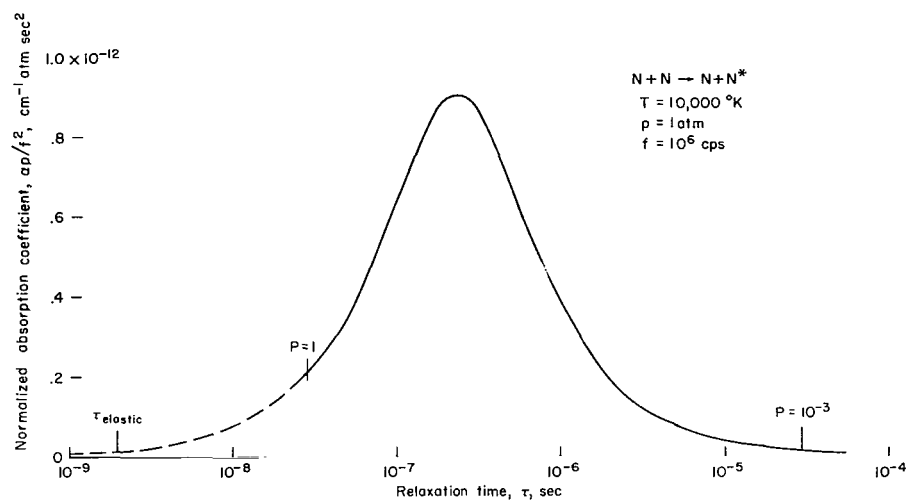


Figure 22.- Effect of collisional excitation time on ultrasonic absorption.

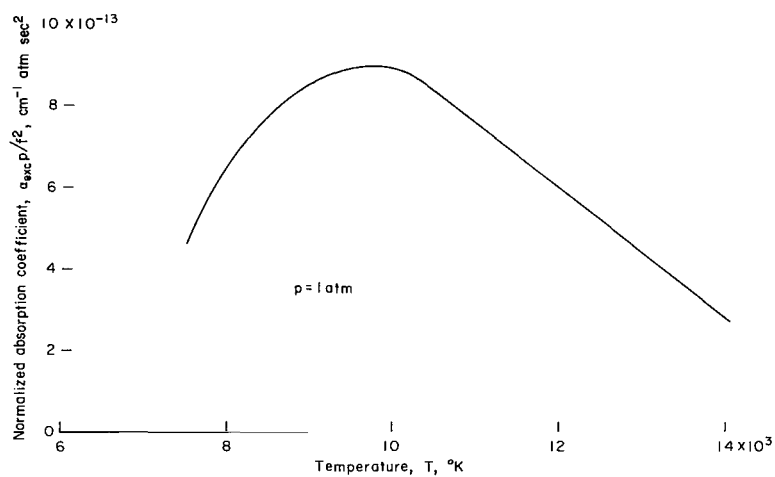


Figure 23.- Temperature variation of ultrasonic absorption due to atomic collisional excitation.

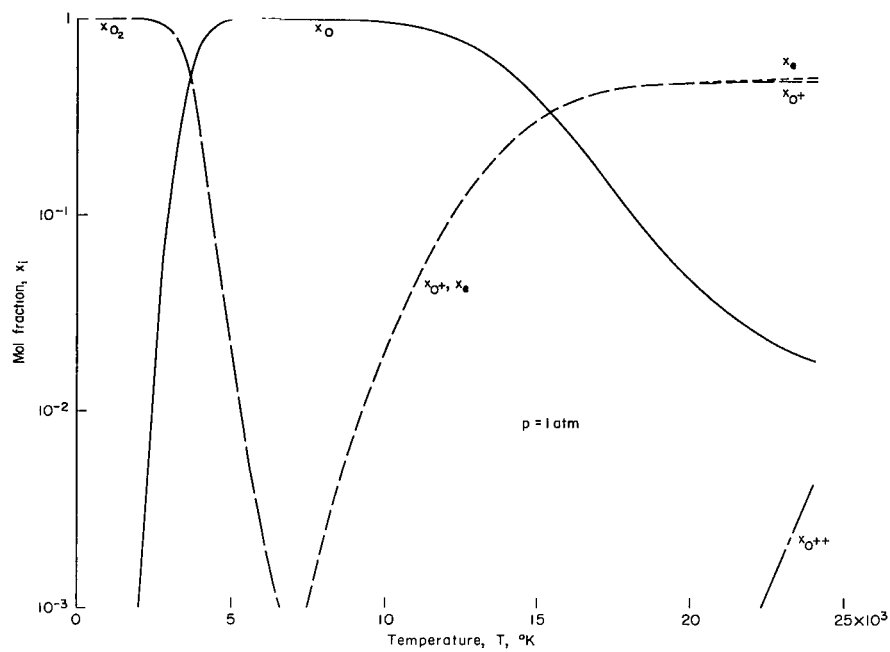


Figure 24.- Mol fraction of species in oxygen.

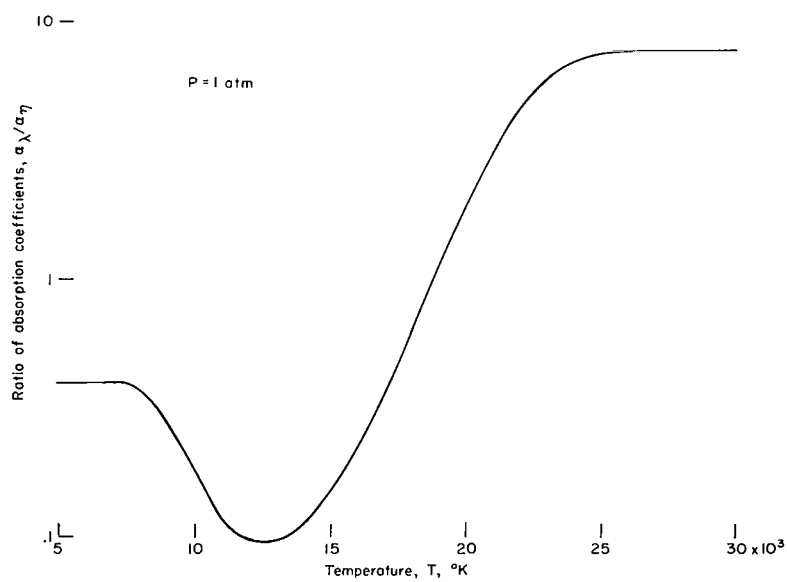


Figure 25.- Comparison of ultrasonic absorption due to thermal conductivity and viscosity in hydrogen.

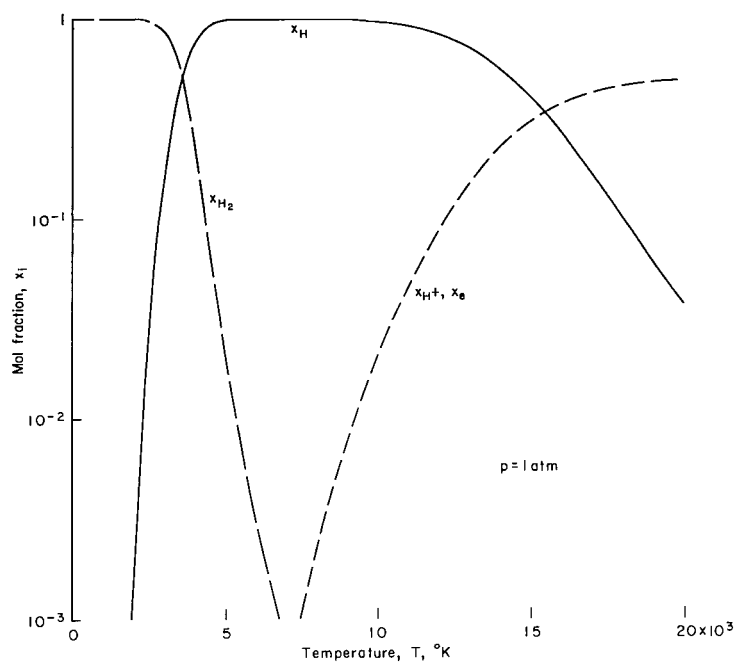


Figure 26.- Mol fraction of species in hydrogen.

070 001 47 02 325 AR0597 00703
AIR FORCE AIRCRAFT DEVELOPMENT/AFWL/
KIRTLAND AIR FORCE BASE, NEW MEXICO 87117

ALL INFORMATION CONTAINED HEREIN IS UNCLASSIFIED
DATE 10/1/01 BY 1047

POSTMASTER: If Undeliverable (Section 158
Postal Manual) Do Not Return

"The aeronautical and space activities of the United States shall be conducted so as to contribute . . . to the expansion of human knowledge of phenomena in the atmosphere and space. The Administration shall provide for the widest practicable and appropriate dissemination of information concerning its activities and the results thereof."

—NATIONAL AERONAUTICS AND SPACE ACT OF 1958

NASA SCIENTIFIC AND TECHNICAL PUBLICATIONS

TECHNICAL REPORTS: Scientific and technical information considered important, complete, and a lasting contribution to existing knowledge.

TECHNICAL NOTES: Information less broad in scope but nevertheless of importance as a contribution to existing knowledge.

TECHNICAL MEMORANDUMS: Information receiving limited distribution because of preliminary data, security classification, or other reasons.

CONTRACTOR REPORTS: Scientific and technical information generated under a NASA contract or grant and considered an important contribution to existing knowledge.

TECHNICAL TRANSLATIONS: Information published in a foreign language considered to merit NASA distribution in English.

SPECIAL PUBLICATIONS: Information derived from or of value to NASA activities. Publications include conference proceedings, monographs, data compilations, handbooks, sourcebooks, and special bibliographies.

TECHNOLOGY UTILIZATION PUBLICATIONS: Information on technology used by NASA that may be of particular interest in commercial and other non-aerospace applications. Publications include Tech Briefs, Technology Utilization Reports and Notes, and Technology Surveys.

Details on the availability of these publications may be obtained from:

SCIENTIFIC AND TECHNICAL INFORMATION DIVISION
NATIONAL AERONAUTICS AND SPACE ADMINISTRATION

Washington, D.C. 20546